

## Exceptional refrigeration of motions beyond their mass and temperature limitations: supplement

**DENG-GAO LAI,<sup>1,2,\*</sup> C.-H. WANG,<sup>1</sup> B.-P. HOU,<sup>1</sup> ADAM MIRANOWICZ,<sup>2,3</sup>  AND FRANCO NORI<sup>2,4,5</sup> **

<sup>1</sup>*College of Physics and Electronic Engineering, Institute of Solid Physics, Sichuan Normal University, Chengdu 610101, China*

<sup>2</sup>*Theoretical Quantum Physics Laboratory, Cluster for Pioneering Research, RIKEN, Wako shi, Saitama 351-0198, Japan*

<sup>3</sup>*Institute of Spintronics and Quantum Information, Faculty of Physics, Adam Mickiewicz University, 61-614 Poznań, Poland*

<sup>4</sup>*Center for Quantum Computing, RIKEN, Wako shi, Saitama 351-0198, Japan*

<sup>5</sup>*Physics Department, University of Michigan, Ann Arbor, Michigan 48109-1040, USA*

\**denggaolai@foxmail.com*

---

This supplement published with Optica Publishing Group on 8 April 2024 by The Authors under the terms of the [Creative Commons Attribution 4.0 License](https://creativecommons.org/licenses/by/4.0/) in the format provided by the authors and unedited. Further distribution of this work must maintain attribution to the author(s) and the published article's title, journal citation, and DOI.

Supplement DOI: <https://doi.org/10.6084/m9.figshare.24992691>

Parent Article DOI: <https://doi.org/10.1364/OPTICA.495199>

## Supplementary Material for

# “Exceptional refrigeration of motions beyond their mass and temperature limitations”

Deng-Gao Lai,<sup>1,2,\*</sup> C.-H. Wang,<sup>1</sup> B.-P. Hou,<sup>1</sup> Adam Miranowicz,<sup>2,3</sup> and Franco Nori<sup>2,4,5</sup>

<sup>1</sup>*College of Physics and Electronic Engineering, Institute of Solid Physics,  
Sichuan Normal University, Chengdu 610101, People’s Republic of China*

<sup>2</sup>*Theoretical Quantum Physics Laboratory, Cluster for Pioneering Research, RIKEN, Wako shi, Saitama 351-0198, Japan*

<sup>3</sup>*Institute of Spintronics and Quantum Information, Faculty of Physics,  
Adam Mickiewicz University, 61-614 Poznań, Poland*

<sup>4</sup>*Center for Quantum Computing, RIKEN, Wako shi, Saitama 351-0198, Japan*

<sup>5</sup>*Physics Department, University of Michigan, Ann Arbor, Michigan 48109-1040, USA*

In this Supplementary Material, we present detailed calculations demonstrating the exceptional refrigeration of vibrations beyond their mass and temperature limitations. Concretely, this document consists of four sections describing : (i) our model Hamiltonian and the analysis of an exceptional point; (ii) the Langevin equations and their solutions for optomechanical networks; (iii) numerical and analytical results of the steady-state mean residual occupation numbers, effective susceptibilities, cooling rates, and noise spectra; and (iv) cooling performance of optomechanical networks.

### I. PHYSICAL MODEL AND ITS EXCEPTIONAL POINT

In this section, we introduce a physical model of optomechanical networks and analyze its exceptional point (EP). Specifically, we consider an EP-assisted optomechanical network, where  $N$  vibrational modes are optomechanically coupled to a common passive cavity, which is linked to an active cavity via a photon-tunneling interaction. A driving laser, with frequency  $\omega_L$  and amplitude  $|\varepsilon_L| = \sqrt{2\kappa_c P_L / \hbar\omega_L}$  (given in terms of the laser power  $P_L$  and the optical decay rate  $\kappa_c$ ), is injected into the loss cavity. The Hamiltonian of the physical system, which is considered in the main text, reads (with  $\hbar = 1$ )

$$H = \omega_c c^\dagger c + \omega_a a^\dagger a + \hbar J(c^\dagger a + ca^\dagger) + \sum_{j=1}^N [\omega_j b_j^\dagger b_j + g_j c^\dagger c(b_j^\dagger + b_j)] + i\varepsilon_L(c^\dagger e^{-i\omega_L t} - ce^{i\omega_L t}). \quad (\text{S1})$$

In the rotating frame, which is defined by the unitary transformation operator  $\exp[-i\omega_L(c^\dagger c + a^\dagger a)t]$ , the Hamiltonian of our optomechanical-network system in Eq. (S1) becomes

$$H_I = \Delta_c c^\dagger c + \Delta_a a^\dagger a + J(c^\dagger a + ca^\dagger) + \sum_{j=1}^N [\omega_j b_j^\dagger b_j + g_j c^\dagger c(b_j^\dagger + b_j)] + i\varepsilon_L(c^\dagger - c), \quad (\text{S2})$$

where the operators  $a^\dagger$  ( $a$ ),  $c^\dagger$  ( $c$ ), and  $b_j^\dagger$  ( $b_j$ ) are, respectively, the creation (annihilation) operators of the gain (active) optical cavity (with resonance frequency  $\omega_a$ ), the loss (passive) cavity (with resonance frequency  $\omega_c$ ), and the  $j$ th vibrational mode (with resonance frequency  $\omega_j$ ). The  $g_j$  terms describe the light-motion interactions between the passive optical mode  $c$  and the  $j$ th motional mode  $b_j$ . Cooling the mechanical resonators to their motional quantum ground states crucially depends on the driving-field strength. The single-photon coupling strength between a single excitation and the  $j$ th vibrational mode scales as  $g_j = \eta_j x_{\text{ZPM},j}$ , where the parameter  $\eta_j$  quantifies the coupling strength to the resonator’s position  $x_j(t)$ , and  $x_{\text{ZPM},j} \sim \sqrt{\hbar/(2m_j\omega_j)}$  is the zero-point motion of the resonator in the trap, with  $\omega_j$  being the vibrational-mode frequency of the center-of-mass. For a large-mass mechanical resonator, a greatly reduced strength  $g_j$  of the light-motion coupling is resulting from the decrease in the zero-point motion  $x_{\text{ZPM},j}$  with increasing the resonator mass  $m_j$ , and this makes its motional quantum ground-state cooling hard to achieve. The photon-tunneling interaction between the loss (passive) and gain (active) optical modes is described by the  $J$  term. The  $\varepsilon_L$  term describes the cavity-field driving, with the parameter  $\Delta_{c(a)} = \omega_{c(a)} - \omega_L$  being the driving detuning for the loss (gain) cavity.

---

\*Electronic address: [denggaolai@foxmail.com](mailto:denggaolai@foxmail.com)

In order to study the EP effect of our optomechanical networks, we here only consider an active-passive optical-cavity configuration, and the dissipation rate  $\kappa_c$  of the passive cavity  $c$  and the gain rate  $\kappa_a$  of the active cavity  $a$  are considered simultaneously. In this case, the effective Hamiltonian of the loss-gain optical-cavity system can be expressed as

$$H_{\text{coupl}} = \omega_c c^\dagger c + \omega_a a^\dagger a - i\kappa_c c^\dagger c + i\kappa_a a^\dagger a + J(c^\dagger a + ca^\dagger). \quad (\text{S3})$$

Note that  $H_{\text{coupl}} = H_c^{\mathcal{PT}}$  is satisfied if and only if both optical cavities are degenerate (i.e.,  $\omega_c = \omega_a = \omega_0$ ), and when the gain rate of the active cavity and decay rate of the passive cavity are balanced (i.e.,  $\kappa_c = \kappa_a$ ), there exists the parity-time ( $\mathcal{PT}$ )-symmetry [S1–S25].

Specifically, by considering the two degenerate optical modes:

$$\omega_c = \omega_a \equiv \omega_0, \quad (\text{S4})$$

and introducing the two supermodes:

$$\mathcal{A}_\pm = (c \pm a)/\sqrt{2}, \quad (\text{S5})$$

we then obtain

$$\mathcal{H}_{\text{coupl}} = \sum_{\pm} \omega_{\pm} \mathcal{A}_{\pm}^{\dagger} \mathcal{A}_{\pm}, \quad (\text{S6})$$

where the corresponding complex eigenvalues are

$$\omega_{\pm} = \omega_0 - i\chi_{\pm} \pm \sqrt{J^2 - \chi_{\pm}^2}, \quad (\text{S7})$$

with

$$\chi_{\pm} = (\kappa_c \pm \kappa_a)/2. \quad (\text{S8})$$

We note that the real and imaginary parts of  $\omega_{\pm}$  are the eigenfrequencies and linewidths, respectively. The system is  $\mathcal{PT}$ -symmetric when this Hamiltonian remains unchanged under both parity-reversal ( $\mathcal{P}$ ) and time-reversal ( $\mathcal{T}$ ) transformations. In this case, a phase transition from the  $\mathcal{PT}$ -symmetric to the broken- $\mathcal{PT}$ -symmetric regimes occurs at the EP [S1–S25].

Specifically, we see from Fig. S1 that, when  $J > \kappa_c$ , the eigenfrequencies have an identical imaginary part and two different real parts. This indicates that the system possesses  $\mathcal{PT}$  symmetry (i.e., the unbroken- $\mathcal{PT}$  symmetry) with an identical linewidth and two different frequencies, as shown in the right-hand side of Fig. S1(a).

In addition, Fig. S1 shows that when  $J < \kappa_c$ , the eigenfrequencies have an identical real part and two different imaginary parts. This means that the linewidths are different and the frequencies of the supermodes are the same, and then the broken- $\mathcal{PT}$ -symmetry occurs i.e., the  $\mathcal{PT}$  symmetry of the system is broken, as shown on the left-hand side of Fig. S1(b).

In particular, it is seen that the phase transition of the  $\mathcal{PT}$  symmetry is clearly exhibited around the border point  $J \approx \kappa_c$ , which is an EP (see the yellow stars in Fig. S1). Here we note that it is a semiclassical EP, corresponding to a spectral degeneracy of a non-Hermitian Hamiltonian. However, for the prediction of a quantum EP, it requires the inclusion of quantum noise by finding degeneracies of, e.g., a Liouvillian, as proposed in Refs. [S4–S6].

## II. LANGEVIN EQUATIONS AND THEIR SOLUTIONS

Based on the Hamiltonian in Eq. (S2), the quantum Langevin equations for the annihilation operators of the two cavity-field modes and  $N$  motional modes can be obtained by phenomenologically adding the dissipation (gain) and quantum noise terms into the Heisenberg equations of motion:

$$\dot{a} = (-i\Delta_a + \kappa_a)a - iJc + \sqrt{2\kappa_a}a_{\text{in}}, \quad (\text{S9a})$$

$$\dot{c} = (-i\Delta_c - \kappa_c)c - iJa - \sum_{j=1}^N ig_j c(b_j^\dagger + b_j) + \varepsilon_L + \sqrt{2\kappa_c}c_{\text{in}}, \quad (\text{S9b})$$

$$\dot{b}_j = (-i\omega_j - \gamma_j)b_j - ig_j c^\dagger c + \sqrt{2\gamma_j}b_{j,\text{in}}, \quad \text{for } j = 1, 2, \dots, N, \quad (\text{S9c})$$

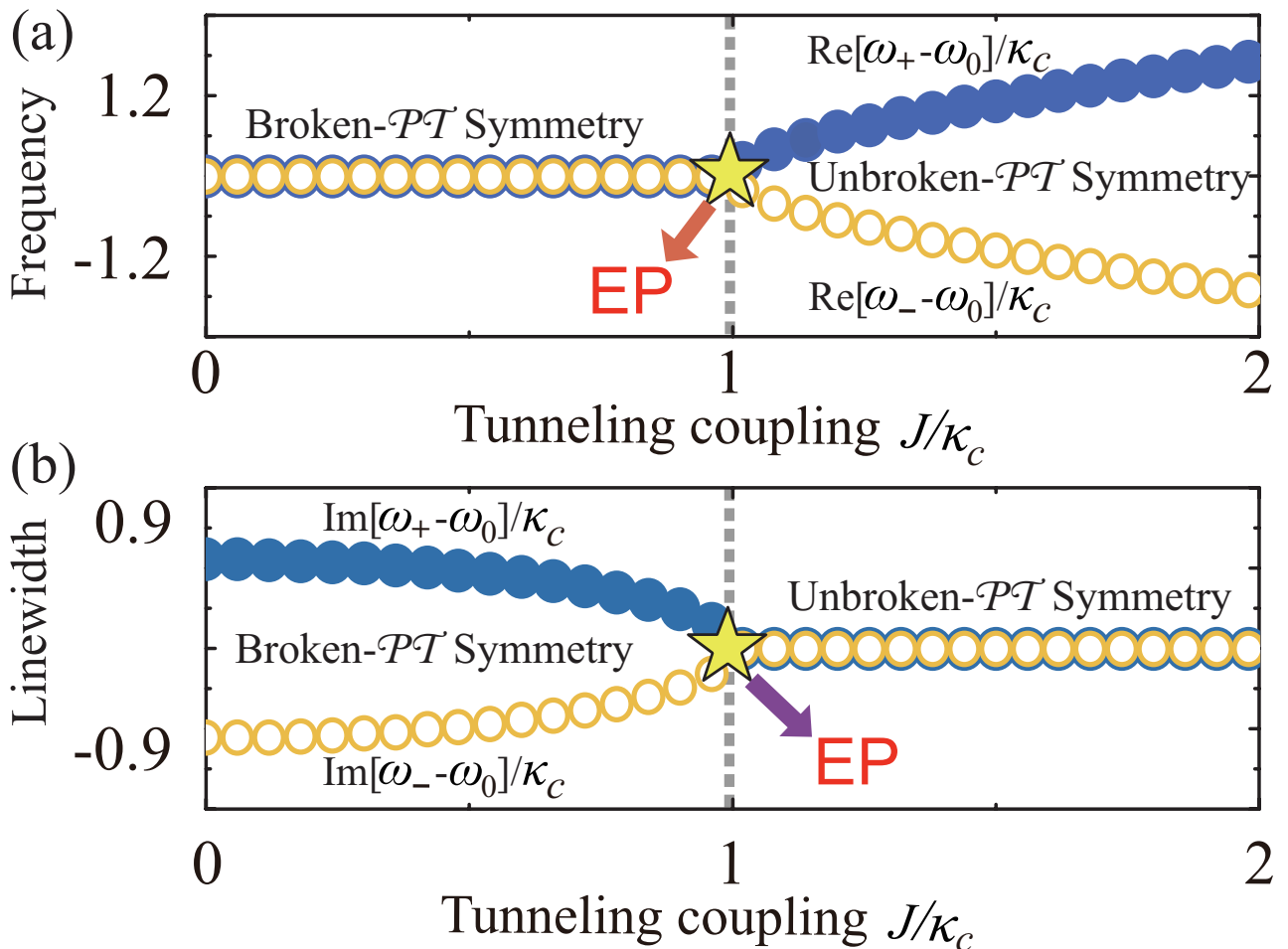


FIG. S1: (a) Real and (b) imaginary parts of  $[\omega_{\pm} - \omega_0]/\kappa_c$  versus the normalized photon-tunneling coupling coefficient  $J/\kappa_c$ . Note that the yellow stars denote the EP. Other parameters are:  $\gamma_1/\omega_1 = \gamma_2/\omega_1 = 10^{-5}$ ,  $\kappa_c/\omega_1 = 1/5\pi$ ,  $\kappa_a/\omega_1 = 1/5\pi$ , and  $\omega_1/2\pi = 20$  MHz.

where  $\kappa_c$  ( $\kappa_a$ ) and  $\gamma_j$  are, respectively, the decay (gain) rates of the passive (active) optical modes and the  $j$ th vibrational mode, while  $c_{\text{in}}$  ( $a_{\text{in}}$ ) and  $b_{j,\text{in}}$  are, respectively, the zero-mean input noise operators for the two optical modes and the  $j$ th motional modes, characterized by the following correlation functions:

$$\langle c_{\text{in}}(t)c_{\text{in}}^\dagger(t') \rangle = \delta(t-t'), \quad (\text{S10a})$$

$$\langle c_{\text{in}}^\dagger(t)c_{\text{in}}(t') \rangle = 0, \quad (\text{S10b})$$

$$\langle b_{j,\text{in}}(t)b_{j,\text{in}}^\dagger(t') \rangle = (\bar{n}_{\text{th},j} + 1)\delta(t-t'), \quad (\text{S10c})$$

$$\langle b_{j,\text{in}}^\dagger(t)b_{j,\text{in}}(t') \rangle = \bar{n}_{\text{th},j}\delta(t-t'), \quad \text{for } j = 1, 2, \dots, N, \quad (\text{S10d})$$

where

$$\bar{n}_{\text{th},j} = \{\exp[\hbar\omega_j/(k_B T_j)] - 1\}^{-1} \quad (\text{S11})$$

is the mean thermal occupation numbers, which are associated with the heat bath of the  $j$ th motional mode, with the parameters  $T_j$  and  $k_B$  being the bath temperature of the  $j$ th vibration and the Boltzmann constant, respectively. In our work, we consider a vacuum bath ( $N_c = 0$ ) for the passive cavity field and a heat bath (with  $\bar{n}_{\text{th},j} \gg 1$ ) for the each mechanical motion. The vacuum bath of the passive cavity field provides the cooling reservoir to absorb the thermal excitations from these mechanical vibrations. But for the active cavity-field mode, the intrinsic quantum

noise is described by the noise operators  $a_{\text{in}}$  and  $a_{\text{in}}^\dagger$ , which satisfy the following correlation functions:

$$\langle a_{\text{in}}(t)a_{\text{in}}^\dagger(t') \rangle = 0, \quad (\text{S12a})$$

$$\langle a_{\text{in}}^\dagger(t)a_{\text{in}}(t') \rangle = \delta(t-t'). \quad (\text{S12b})$$

In order to cool the mechanical vibrations of the optomechanical networks, the strong-driving regime of the passive cavity is considered, such that the mean photon number in this passive cavity is sufficiently large. Then, we can use a linearization procedure to simplify the physical model of the optomechanical networks. Specifically, the operators in Eq. (S9) can be expressed as the sums of their steady-state mean values and quantum fluctuations, i.e.,

$$a = \alpha_1 + \delta a, \quad (\text{S13a})$$

$$c = \alpha_2 + \delta c, \quad (\text{S13b})$$

$$b_j = \beta_j + \delta b_j \quad \text{for } j = 1, 2, \dots, N. \quad (\text{S13c})$$

By separating the steady-state mean values from quantum fluctuations, and ignoring all the higher-order terms of quantum fluctuations, the linearized equations of motion of quantum fluctuations and the steady-state equations of the quantum Langevin equations can be obtained, respectively. Thus, we obtain the linearized equations of motion of quantum fluctuations, which are given by

$$\frac{d}{dt}\delta a = (-i\Delta_2 + \kappa_a)\delta a - iJ\delta c + \sqrt{2\kappa_a}a_{\text{in}}, \quad (\text{S14a})$$

$$\frac{d}{dt}\delta c = (-i\Delta_1 - \kappa_c)\delta c - iJ\delta a - i\sum_{j=1}^N G_j(\delta b_j^\dagger + \delta b_j) + \sqrt{2\kappa_c}c_{\text{in}}, \quad (\text{S14b})$$

$$\frac{d}{dt}\delta b_j = (-i\omega_j - \gamma_j)\delta b_j - iG_j^*\delta c - iG_j\delta c^\dagger + \sqrt{2\gamma_j}b_{j,\text{in}} \quad \text{for } j = 1, 2, \dots, N, \quad (\text{S14c})$$

where

$$\Delta_1 = \Delta_c + \sum_{j=1}^N g_j(\beta_j^* + \beta_j) \quad (\text{S15})$$

and  $\Delta_2 = \Delta_a$  are, respectively, the effective detunings of the passive and active optical cavities, and the parameter  $G_j = g_j\alpha_2$  denotes the effective optomechanical-coupling strength between the  $j$ th vibrational mode and the passive cavity. For simplicity, in the following discussions, we consider the case where  $\alpha_2$  is real, which can be experimentally done by choosing a proper driving amplitude  $\epsilon_L$ . Thus, the linearized optomechanical coupling strengths  $G_j$  are real. Hereafter, we consider the case of  $\Delta_1 \approx \Delta_2 \approx \Delta$ .

Meanwhile, we obtain the equations of motion for the classical motion variables:

$$\frac{d}{dt}\alpha_1 = (-i\Delta_a + \kappa_a)\alpha_1 - iJ\alpha_2, \quad (\text{S16a})$$

$$\frac{d}{dt}\alpha_2 = (-i\Delta_c - \kappa_c)\alpha_2 - iJ\alpha_1 - \sum_{j=1}^N ig_j\alpha_2(\beta_j^* + \beta_j) + \epsilon_L, \quad (\text{S16b})$$

$$\frac{d}{dt}\beta_j = (-i\omega_j - \gamma_j)\beta_j - ig_j\alpha_2^*\alpha_2, \quad \text{for } j = 1, 2, \dots, N. \quad (\text{S16c})$$

In our work, we focus only on the steady state of the quantum system and, thus, we set all the left-hand sides of Eq. (S16) equal to zero:

$$0 = (-i\Delta_a + \kappa_a)\alpha_1 - iJ\alpha_2, \quad (\text{S17a})$$

$$0 = (-i\Delta_c - \kappa_c)\alpha_2 - iJ\alpha_1 - \sum_{j=1}^N ig_j\alpha_2(\beta_j^* + \beta_j) + \epsilon_L, \quad (\text{S17b})$$

$$0 = (-i\omega_j - \gamma_j)\beta_j - ig_j\alpha_2^*\alpha_2, \quad \text{for } j = 1, 2, \dots, N. \quad (\text{S17c})$$

Then the steady-state average values of the dynamical variables of quantum optomechanical networks are obtained as:

$$\alpha_1 = \frac{-iJ\alpha_2}{(i\Delta_a - \kappa_a)}, \quad (\text{S18a})$$

$$\alpha_2 = \frac{-iJ\alpha_1 + \varepsilon_L}{\kappa_c + i \left[ \Delta_c + \sum_{j=1}^N g_j(\beta_j^* + \beta_j) \right]} = \frac{-iJ\alpha_1 + \varepsilon_L}{\kappa_c + i\Delta_1}, \quad (\text{S18b})$$

$$\beta_j = \frac{-ig_j\alpha_2^*\alpha_2}{i\omega_j + \gamma_j}, \quad \text{for } j = 1, 2, \dots, N, \quad (\text{S18c})$$

where the parameter  $\Delta_1 = \Delta_c + \sum_{j=1}^N g_j(\beta_j^* + \beta_j)$ . In order to study the refrigeration performance of the optomechanical networks, we need to evaluate the steady-state mean occupation numbers in the  $N$  mechanical motions. To this end, the linearized quantum Langevin equations in (S14) can be safely written in the following compact form:

$$\dot{\mathbf{u}}(t) = \mathbf{A}\mathbf{u}(t) + \mathbf{N}(t), \quad (\text{S19})$$

where the fluctuation-operator vector  $\mathbf{u}(t)$ , the noise operator vector  $\mathbf{N}(t)$ , and the coefficient matrix  $\mathbf{A}$  are, respectively, defined as:

$$\mathbf{u}(t) = (\delta c, \delta c^\dagger, \delta a, \delta a^\dagger, \delta b_1, \delta b_1^\dagger, \delta b_2, \delta b_2^\dagger, \dots, \delta b_{N-1}, \delta b_{N-1}^\dagger, \delta b_N, \delta b_N^\dagger)^T, \quad (\text{S20})$$

$$\mathbf{N}(t) = \sqrt{2}(\sqrt{\kappa_c}c_{\text{in}}, \sqrt{\kappa_c}c_{\text{in}}^\dagger, \sqrt{\kappa_a}a_{\text{in}}, \sqrt{\kappa_a}a_{\text{in}}^\dagger, \sqrt{\gamma_1}b_{1,\text{in}}, \sqrt{\gamma_1}b_{1,\text{in}}^\dagger, \sqrt{\gamma_2}b_{2,\text{in}}, \sqrt{\gamma_2}b_{2,\text{in}}^\dagger, \dots, \sqrt{\gamma_N}b_{N,\text{in}}, \sqrt{\gamma_N}b_{N,\text{in}}^\dagger)^T, \quad (\text{S21})$$

and

$$\mathbf{A} = \begin{pmatrix} -i\Delta - \kappa_c & 0 & -iJ & 0 & -iG_1 & -iG_1 & -iG_2 & -iG_2 & -iG_3 & -iG_3 & \cdots & -iG_N & -iG_N \\ 0 & i\Delta - \kappa_c & 0 & iJ & iG_1^* & iG_1^* & iG_2^* & iG_2^* & iG_3^* & iG_3^* & \cdots & iG_N^* & iG_N^* \\ -iJ & 0 & -i\Delta + \kappa_a & 0 & 0 & 0 & 0 & 0 & 0 & 0 & \cdots & 0 & 0 \\ 0 & iJ & 0 & i\Delta + \kappa_a & 0 & 0 & 0 & 0 & 0 & 0 & \cdots & 0 & 0 \\ -iG_1^* & -iG_1 & 0 & 0 & -i\omega_1 - \gamma_1 & 0 & 0 & 0 & 0 & 0 & \cdots & 0 & 0 \\ iG_1^* & iG_1 & 0 & 0 & 0 & i\omega_1 - \gamma_1 & 0 & 0 & 0 & 0 & \cdots & 0 & 0 \\ -iG_2^* & -iG_2 & 0 & 0 & 0 & 0 & -i\omega_2 - \gamma_2 & 0 & 0 & 0 & \cdots & 0 & 0 \\ iG_2^* & iG_2 & 0 & 0 & 0 & 0 & 0 & i\omega_2 - \gamma_2 & 0 & 0 & \cdots & 0 & 0 \\ -iG_3^* & -iG_3 & 0 & 0 & 0 & 0 & 0 & 0 & -i\omega_3 - \gamma_3 & 0 & \cdots & 0 & 0 \\ iG_3^* & iG_3 & 0 & 0 & 0 & 0 & 0 & 0 & 0 & i\omega_3 - \gamma_3 & \cdots & 0 & 0 \\ \vdots & \ddots & \vdots & \vdots \\ -iG_N^* & -iG_N & 0 & 0 & 0 & 0 & 0 & 0 & 0 & 0 & \cdots & -i\omega_N - \gamma_N & 0 \\ iG_N^* & iG_N & 0 & 0 & 0 & 0 & 0 & 0 & 0 & 0 & \cdots & 0 & i\omega_N - \gamma_N \end{pmatrix}. \quad (\text{S22})$$

Then, we can write the formal solution of the linearized Langevin equation (S19) as

$$\mathbf{u}(t) = \mathbf{M}(t)\mathbf{u}(0) + \int_0^t \mathbf{M}(t-s)\mathbf{N}(s)ds, \quad (\text{S23})$$

where the matrix  $\mathbf{M}(t)$  is defined as:

$$\mathbf{M}(t) = \exp(\mathbf{A}t), \quad (\text{S24})$$

with the coefficient matrix  $\mathbf{A}$  given in Eq. (S22).

### III. NUMERICAL AND ANALYTICAL RESULTS FOR THE FINAL MEAN RESIDUAL OCCUPATION NUMBERS, EFFECTIVE SUSCEPTIBILITIES, COOLING RATES, AND NOISE SPECTRA

In this section, we focus on finding both numerical and analytical expressions of the final mean occupation numbers of the  $N$  mechanical vibrations, and deriving analytical expressions of the effective susceptibilities, cooling rates, and noise spectra.

### A. Numerical results for the final mean residual thermal occupation numbers

Based on the formal solution of the linearized Langevin equation shown in Sec. II, we can calculate the steady-state average thermal occupation numbers of the  $N$  mechanical vibrations by solving the Lyapunov equation. Here we need to emphasize that all the parameters, used in the following calculations, satisfy the stability conditions derived from the Routh-Hurwitz criterion [S26]; namely, the real parts of all the eigenvalues of the coefficient matrix  $\mathbf{A}$  are negative.

For studying quantum optomechanical refrigeration of the  $N$  motional modes, we focus on the steady-state average thermal occupation numbers in the  $N$  mechanical vibrations, by calculating the steady-state value of the covariance matrix  $\mathbf{V}$ , with the elements:

$$\mathbf{V}_{ij} = \frac{1}{2}[\langle \mathbf{u}_i(\infty)\mathbf{u}_j(\infty) \rangle + \langle \mathbf{u}_j(\infty)\mathbf{u}_i(\infty) \rangle], \quad \text{for } i, j = 1, \dots, (2N+4). \quad (\text{S25})$$

In our linearized optomechanical system, the covariance matrix  $\mathbf{V}$  satisfies the Lyapunov equation,

$$\mathbf{A}\mathbf{V} + \mathbf{V}\mathbf{A}^T = -\mathbf{Q}, \quad (\text{S26})$$

where the superscript  $T$  is the matrix transpose operation, and the matrix  $\mathbf{Q}$  is defined as

$$\mathbf{Q} = \frac{1}{2}(\mathbf{C} + \mathbf{C}^T), \quad (\text{S27})$$

with  $\mathbf{C}$  being the noise correlation matrix, with the elements:

$$\langle \mathbf{N}_k(s)\mathbf{N}_l(s') \rangle = \mathbf{C}_{k,l}\delta(s-s'). \quad (\text{S28})$$

For the Markovian baths considered in our work, we obtain the constant matrix  $\mathbf{C}$ , given by

$$\mathbf{C} = \begin{pmatrix} 0 & 2\kappa_c & 0 & 0 & 0 & 0 & 0 & 0 & 0 & 0 & \dots & 0 & 0 \\ 0 & 0 & 0 & 0 & 0 & 0 & 0 & 0 & 0 & 0 & \dots & 0 & 0 \\ 0 & 0 & 0 & 0 & 0 & 0 & 0 & 0 & 0 & 0 & \dots & 0 & 0 \\ 0 & 0 & 2\kappa_a & 0 & 0 & 0 & 0 & 0 & 0 & 0 & \dots & 0 & 0 \\ 0 & 0 & 0 & 0 & 0 & 2\gamma_1(\bar{n}_1+1) & 0 & 0 & 0 & 0 & \dots & 0 & 0 \\ 0 & 0 & 0 & 0 & 2\gamma_1\bar{n}_1 & 0 & 0 & 0 & 0 & 0 & \dots & 0 & 0 \\ 0 & 0 & 0 & 0 & 0 & 0 & 2\gamma_2(\bar{n}_2+1) & 0 & 0 & 0 & \dots & 0 & 0 \\ 0 & 0 & 0 & 0 & 0 & 0 & 2\gamma_2\bar{n}_2 & 0 & 0 & 0 & \dots & 0 & 0 \\ 0 & 0 & 0 & 0 & 0 & 0 & 0 & 0 & 2\gamma_3(\bar{n}_3+1) & \dots & 0 & 0 & 0 \\ 0 & 0 & 0 & 0 & 0 & 0 & 0 & 0 & 2\gamma_3\bar{n}_3 & 0 & \dots & 0 & 0 \\ \vdots & \ddots & \vdots & \vdots & \vdots \\ 0 & 0 & 0 & 0 & 0 & 0 & 0 & 0 & 0 & \dots & 0 & 2\gamma_N(\bar{n}_N+1) & 0 \\ 0 & 0 & 0 & 0 & 0 & 0 & 0 & 0 & 0 & \dots & 2\gamma_N\bar{n}_N & 0 & 0 \end{pmatrix}. \quad (\text{S29})$$

By applying the covariance matrix  $\mathbf{V}$ , we derive the final residual mean number of thermal quanta in the  $j$ th mechanical vibration:

$$n_{j \in [1, N]}^f = \mathbf{V}_{(2j+4)(2j+3)} - \frac{1}{2}, \quad \text{for } j = 1, 2, \dots, N, \quad (\text{S30})$$

where  $\mathbf{V}_{(2j+4)(2j+3)}$  can be obtained by solving the Lyapunov equation in Eq. (S26).

### B. Analytical results for the effective susceptibilities, cooling rates, and noise spectra

In order to study the refrigeration performance of all the mechanical vibrations, we need to obtain the effective susceptibilities, cooling rates, and noise spectra in the optomechanical system. For convenience, we introduce the position and momentum operators of the  $j$ th vibrational mode:

$$x_j = \sqrt{\frac{\hbar}{2m_j\omega_j}}(b_j^\dagger + b_j), \quad (\text{S31a})$$

$$p_{x_j} = i\sqrt{\frac{m_j\hbar\omega_j}{2}}(b_j^\dagger - b_j), \quad (\text{S31b})$$

which satisfy the bosonic commutation relation: i.e.,  $[x_j, p_{x_j}] = i\hbar$ , where  $m_j$  and  $\omega_j$  are its mass and resonance frequency. Then, by using the presentation of the position and momentum operators of the mechanical vibrations, the Hamiltonian of our quantum system becomes ( $\hbar = 1$ )

$$H_0 = \omega_c c^\dagger c + \omega_a a^\dagger a + \sum_{j=1}^2 \left( \frac{p_{x_j}^2}{2m_j} + \frac{m_j \omega_j^2 x_j^2}{2} \right) + J(c^\dagger a + ca^\dagger) + \sum_{j=1}^2 \lambda_j c^\dagger c x_j + i\varepsilon_L (c^\dagger e^{-i\omega_L t} - c e^{i\omega_L t}), \quad (\text{S32})$$

where  $c$  ( $c^\dagger$ ) and  $a$  ( $a^\dagger$ ) represent the annihilation (creation) operators of the passive and active cavity-field modes with the optical resonance frequencies  $\omega_c$  and  $\omega_a$ , respectively. The  $\lambda_j$  term describes the radiation-pressure coupling between the  $j$ th mechanical oscillator and the optical cavity  $c$ , and the  $J$  term denotes the photon-hopping interaction between the two optical cavities. The  $\varepsilon_L = \sqrt{2P_L \kappa_c / \omega_L}$  term is the optical driving of the system, with  $P_L$  being the driving laser power, and  $\kappa_c$  being the decay rate of the lossy cavity  $c$ .

For convenience, we below introduce the dimensionless coordinate operator

$$q_j = \sqrt{m_j \omega_j} x_j, \quad (\text{S33})$$

and the dimensionless momentum operator

$$p_j = \sqrt{1/(m_j \omega_j)} p_{x_j}, \quad (\text{S34})$$

with  $[q_j, p_j] = i$ . By defining the unitary transformation operator

$$U(t) = \exp[-i\omega_L (c^\dagger c + a^\dagger a)t], \quad (\text{S35})$$

the Hamiltonian of the system becomes

$$H_1 = \Delta_c c^\dagger c + \Delta_a a^\dagger a + \sum_{j=1}^2 \left[ \frac{\omega_j}{2} (p_j^2 + q_j^2) + \lambda_{0j} c^\dagger c q_j \right] + J(c^\dagger a + ca^\dagger) + i\varepsilon_L (c^\dagger - c), \quad (\text{S36})$$

where

$$\lambda_{0j} = \lambda_j / \sqrt{m_j \omega_j} \quad (\text{S37})$$

is the dimensionless optomechanical-coupling strength, and

$$\Delta_c = \omega_c - \omega_L, \quad (\text{S38})$$

$$\Delta_a = \omega_a - \omega_L, \quad (\text{S39})$$

denote the effective detunings of the lossy-cavity and gain-cavity fields, respectively.

By phenomenologically adding the damping (gain) and noise terms into the Heisenberg equations obtained using the Hamiltonian in Eq. (S36), the quantum Langevin equations for the operators of all the optical and mechanical modes can be obtained as:

$$\dot{a} = (\kappa_a + i\Delta_a)a - iJc + \sqrt{2\kappa_a}a_{\text{in}}, \quad (\text{S40a})$$

$$\dot{c} = -[\kappa_c + i(\Delta_c + \lambda_{01}q_1 + \lambda_{02}q_2)]c - iJa + \varepsilon_L + \sqrt{2\kappa_c}c_{\text{in}}, \quad (\text{S40b})$$

$$\dot{p}_j = -\omega_j q_j - \lambda_{0j} c^\dagger c - \gamma_j p_j + \xi_j, \quad (\text{S40c})$$

$$\dot{q}_j = \omega_j p_j, \quad (\text{S40d})$$

where  $\kappa_c$  ( $\kappa_a$ ) and  $\gamma_j$  are the loss (gain) rate of the lossy (gain) optical cavity and the decay rate of the two mechanical oscillators, respectively. The operators  $c_{\text{in}}$  and  $a_{\text{in}}$  denote the input noise operators of the two cavity fields, and  $\xi_j$  denotes the Brownian noise operator generated by the corresponding vibrational modes coupled to the thermal bath,

which have zero average value and are represented by the following correlation functions:

$$\langle c_{\text{in}}(t)c_{\text{in}}^\dagger(t') \rangle = \delta(t-t'), \quad (\text{S41a})$$

$$\langle c_{\text{in}}^\dagger(t)c_{\text{in}}(t') \rangle = 0, \quad (\text{S41b})$$

$$\langle a_{\text{in}}(t)a_{\text{in}}^\dagger(t') \rangle = 0, \quad (\text{S41c})$$

$$\langle a_{\text{in}}^\dagger(t)a_{\text{in}}(t') \rangle = \delta(t-t'), \quad (\text{S41d})$$

$$\langle \xi_j(t)\xi_j(t') \rangle = \frac{\gamma_j}{\omega_j} \int \frac{d\omega}{2\pi} e^{-i\omega(t-t')} \omega \left[ 1 + \coth\left(\frac{\omega}{2K_B T_j}\right) \right]. \quad (\text{S41e})$$

Here, we consider the lossy cavity  $c$  driven by a strong driving laser, and, thus, by using the standard linearization method of quantum optics, all the variables of the system can be expressed as the sums of the steady-state average and the quantum fluctuation, i.e.,

$$A = \langle A \rangle_{ss} + \delta A, \quad (\text{S42})$$

where  $A = c, c^\dagger, a, a^\dagger, q_j$ , and,  $p_j$ . In order to derive analytical expressions of the final mean phonon numbers and net-cooling rates, we here need to introduce the orthogonal operators, defined as:

$$\delta X_o = (\delta o^\dagger + \delta o)/\sqrt{2}, \quad (\text{S43a})$$

$$\delta Y_o = i(\delta o^\dagger - \delta o)/\sqrt{2}, \quad (\text{S43b})$$

for the operators  $o = a$  and  $c$ . In Eq. (S40), by separating the steady states from the quantum fluctuations and after ignoring all the high-order terms, the equations of motion of the quantum fluctuations can be linearized and expressed as

$$\delta \dot{X}_a = \kappa_a \delta X_a - \Delta_{c2} \delta Y_a + J \delta Y_c + \sqrt{2\kappa_a} X_{a,\text{in}}, \quad (\text{S44a})$$

$$\delta \dot{Y}_a = \kappa_a \delta Y_a + \Delta_{c2} \delta X_a - J \delta X_c + \sqrt{2\kappa_a} Y_{a,\text{in}}, \quad (\text{S44b})$$

$$\delta \dot{X}_c = -\kappa_c \delta X_c + \Delta \delta Y_c + J \delta Y_a + \frac{i\sqrt{2}}{2} (G_1^\dagger - G_1) \delta q_1 + \frac{i\sqrt{2}}{2} (G_2^\dagger - G_2) \delta q_2 + \sqrt{2\kappa_c} X_{c,\text{in}}, \quad (\text{S44c})$$

$$\delta \dot{Y}_c = -\kappa_c \delta Y_c - \Delta X_c - J \delta X_a - \frac{\sqrt{2}}{2} (G_1^\dagger + G_1) \delta q_1 - \frac{\sqrt{2}}{2} (G_2^\dagger + G_2) \delta q_2 + \sqrt{2\kappa_c} Y_{c,\text{in}}, \quad (\text{S44d})$$

$$\delta \dot{p}_j = -\omega_j \delta q_j - \frac{\sqrt{2}}{2} (G_j^\dagger + G_j) \delta X_c - \frac{i\sqrt{2}}{2} (G_j^\dagger - G_j) \delta Y_c - \gamma_j \delta p_j + \xi_j, \quad (\text{S44e})$$

$$\delta \dot{q}_j = \omega_j \delta p_j, \quad (\text{S44f})$$

where

$$\Delta = \Delta_c + \sum_{j=1}^2 \lambda_{0j} \langle q_j \rangle_{ss} \quad (\text{S45})$$

represents the effective driving detuning after performing the linearization, and we here assume  $\Delta_a = \Delta_2$ . The parameters  $G_1 = \lambda_{01} \langle c \rangle_{ss}$  and  $G_2 = \lambda_{02} \langle c \rangle_{ss}$  are, respectively, the linearized optomechanical-coupling intensities of the passive optical mode and the two mechanical modes. The operators

$$X_{o,\text{in}} = \frac{1}{\sqrt{2}} (o_{o,\text{in}}^\dagger + o_{o,\text{in}}), \quad (\text{S46a})$$

$$Y_{o,\text{in}} = \frac{i}{\sqrt{2}} (o_{o,\text{in}}^\dagger - o_{o,\text{in}}), \quad \text{for } o = a, c, \quad (\text{S46b})$$

are the corresponding Hermitian input-noise orthogonal operators. In addition, we obtain the steady-state solution

of the quantum Langevin equation, given by

$$\langle a \rangle_{ss} = \frac{iJ\langle c \rangle_{ss}}{\kappa_a - i\Delta_2}, \quad (\text{S47a})$$

$$\langle c \rangle_{ss} = \frac{-iJ\langle a \rangle_{ss} + \varepsilon_L}{\kappa_c + i\Delta}, \quad (\text{S47b})$$

$$\langle q_1 \rangle_{ss} = \frac{-\lambda_{01}\langle c^\dagger \rangle_{ss}\langle c \rangle_{ss}}{\omega_1}, \quad (\text{S47c})$$

$$\langle q_2 \rangle_{ss} = \frac{-\lambda_{02}\langle c^\dagger \rangle_{ss}\langle c \rangle_{ss}}{\omega_2}, \quad (\text{S47d})$$

$$\langle p_1 \rangle_{ss} = \langle p_2 \rangle_{ss} = 0. \quad (\text{S47e})$$

In the next step, we derive the analytical expressions of the effective mechanical susceptibilities, net-refrigeration rates, and noise spectra, and study the cooling performance of these vibrational modes. To this end, we obtain the fluctuation spectra of the position and momentum of these mechanical motions, defined by

$$S_o(\omega) = \int_{-\infty}^{\infty} e^{-i\omega\tau} \langle \delta o(t+\tau)\delta o(t) \rangle_{ss} d\tau, \quad (\text{S48})$$

for  $o = q_j$  and  $p_j$ . Here  $\langle \cdot \rangle_{ss}$  is taken over the steady state of the system. In addition, the fluctuation spectra of the system can be expressed in the frequency domain as

$$\langle \delta \tilde{o}(\omega)\delta \tilde{o}(\omega') \rangle_{ss} = S_o(\omega)\delta(\omega + \omega'), \quad (o = q_j, p_j). \quad (\text{S49})$$

By using the results given in Eqs. (S44) and (S48), and the correlation functions in Eq. (S49) in the frequency domain, we obtain the position fluctuation spectra of these vibrational modes as:

$$S_{q_j}(\omega) = |\chi_{j,\text{eff}}(\omega)|^2 [S_{\text{rp},j}(\omega) + S_{\text{th},j}(\omega) + S_{\text{EP},j}(\omega)]. \quad (\text{S50})$$

Based on the position-fluctuation spectra shown in Eq. (S50), the effective susceptibilities of the  $j$ th motional mode can be obtained as

$$\chi_{j,\text{eff}}(\omega) = \omega_j [\Omega_{j,\text{eff}}^2(\omega) - \omega^2 - i\omega\Gamma_{j,\text{eff}}(\omega)]^{-1}, \quad (\text{S51})$$

where the parameter  $\Gamma_{j,\text{eff}}(\omega)$  denotes the effective mechanical decay rate of the  $j$ th vibrational mode, defined as:

$$\Gamma_{j,\text{eff}}(\omega) = \gamma_j + \gamma_{j,\text{C}}(\omega), \quad (\text{S52})$$

and the parameter  $\Omega_{j,\text{eff}}(\omega)$  is the effective mechanical resonance frequency of the  $j$ th motional mode, defined as

$$\Omega_{j,\text{eff}}(\omega) = \omega_j + \delta\omega_j(\omega). \quad (\text{S53})$$

In Eq. (S52), the parameter  $\gamma_{j,\text{C}}$  denotes the net-refrigeration rate of the  $j$ th motional mode, which is given by

$$\gamma_{1,\text{C}} = \frac{D_3(\omega)}{B_5^2(\omega) + B_6^2(\omega)}, \quad (\text{S54a})$$

$$\gamma_{2,\text{C}} = \frac{L_3(\omega)}{F_5^2(\omega) + F_6^2(\omega)}. \quad (\text{S54b})$$

In cavity optomechanics, the optomechanical-cooling rate can be obtained by calculating: (i) the anti-Stokes/Stokes scattering rates [S28, S29], and (ii) the effective mechanical decay rate [S30]. In our work, we use the second method to obtain the effective mechanical susceptibility, and then to find the frequency-dependent effective mechanical damping, corresponding to the sum of the net-cooling rate and the mechanical decay rate (the coupling rate with the thermal reservoir). It has been confirmed that the optimal Fourier frequency  $\omega$  is located around the resonance  $\omega \approx \omega_1$ , corresponding to an optimal cooling net. In fact, the cooling rates are evaluated by considering the Fourier frequency  $\omega$  close to the bare mechanical-mode resonance  $\omega_1$ , and this is often done in cavity optomechanics.

Here we show an intuitive picture and to facilitate the comparison with the recent perturbation treatments of Refs. [S28, S29], where photons are simultaneously scattered by the mechanical vibration with the emission (with an anti-Stokes-scattering rate) or the absorption (with a Stokes-scattering rate) of phonons. As a result, the net-cooling rate based on Refs. [S28, S29] is equal to the difference between the antiStokes- and Stokes-scattering rates.

Correspondingly, the net-cooling rate in our method corresponds to the difference of the effective mechanical decay rate and the mechanical damping rate, in agreement with Eq. (S52). The quantum ground-state cooling can be achieved, when  $\gamma_j$  (the coupling rate with the thermal reservoir) is significantly smaller than the net-cooling rate  $\gamma_{j,C}$ , representing the coupling rate of the mechanical resonator with the effective reservoir provided by the damped cavity mode.

The parameter  $\delta\omega_j(\omega)$  in Eq. (S53) is the mechanical frequency shift of the  $j$ th motional mode, which is caused by the optical spring effect and given by

$$\delta\omega_1 = \sqrt{\omega_1^2 - \frac{D_1(\omega)}{B_5^2(\omega) + B_6^2(\omega)}} - \omega_1, \quad (\text{S55a})$$

$$\delta\omega_2 = \sqrt{\omega_2^2 - \frac{L_1(\omega)}{F_5^2(\omega) + F_6^2(\omega)}} - \omega_2, \quad (\text{S55b})$$

where the parameters  $A_{j=1,\dots,10}$  are defined as:

$$\begin{aligned} A_1 &= J^4(\omega_2^2 - \omega^2), & A_2 &= \gamma_2\omega J^4, \\ A_3 &= \Delta_2^2 + \kappa_a^2 - \omega^2, & A_4 &= 2\kappa_a\omega, \\ A_5 &= -2\gamma_2\kappa_c\omega^2 - 2G_2^2\Delta\omega_2 - (\kappa_c^2 - \omega^2)(\omega^2 - \omega_2^2) + \Delta^2(\omega_2^2 - \omega^2), \\ A_6 &= \omega(-\gamma_2(\Delta^2 + \kappa_c^2 - \omega^2) + 2\kappa_c(\omega^2 - \omega_2^2)), \\ A_7 &= \omega^2(\Delta\Delta_2 - \gamma_2\kappa_c + (\gamma_2 + \kappa_c)\kappa_a + \omega^2) + G_2^2\Delta_2\omega_2, \\ A_8 &= \gamma_2(\Delta\Delta_2 + \kappa_c\kappa_a)\omega + (\gamma_2 + \kappa_c - \kappa_2)\omega^3, \\ A_9 &= (\Delta\Delta_2 + \kappa_c\kappa_a + \omega^2)\omega_2^2, & A_{10} &= (\kappa_c - \kappa_a)\omega\omega_2^2, \end{aligned} \quad (\text{S56})$$

the parameters  $B_{j=1,\dots,6}$  are:

$$\begin{aligned} B_1 &= A_3A_5 - A_4A_6, & B_2 &= A_4A_5 + A_3A_6, \\ B_3 &= 2J^2(A_7 - A_9), & B_4 &= 2J^2(A_8 - A_{10}), \\ B_5 &= A_1 + B_1 + B_3, & B_6 &= B_2 + B_4 - A_2, \end{aligned} \quad (\text{S57})$$

the parameters  $C_{j=1,\dots,6}$  take the form:

$$\begin{aligned} C_1 &= 2G_1^2(J^2\Delta_2 - \Delta(\Delta_2^2 + \kappa_a^2 - \omega^2)), \\ C_2 &= -4G_1^2\Delta\kappa_a\omega, & C_3 &= (\omega^2 - \omega_2^2)\omega_1, \\ C_4 &= \gamma_2\omega\omega_1, & C_5 &= C_1C_3 - C_2C_4, \\ C_6 &= C_2C_3 + C_1C_4, \end{aligned} \quad (\text{S58})$$

the parameters  $D_{j=1,2,3}$ ,  $E_{j=1,\dots,9}$ , and  $F_{j=1,\dots,6}$  are:

$$\begin{aligned} D_1 &= B_5C_5 + B_6C_6, & D_2 &= B_5C_6 + B_6C_5, \\ E_1 &= J^4(\omega_1^2 - \omega^2), & E_2 &= \gamma_1\omega J^4, \\ E_3 &= \Delta_2^2 + \kappa_a^2 - \omega^2, & E_4 &= 2\kappa_a\omega, \\ E_5 &= -2\gamma_1\kappa_c\omega^2 - 2G_1^2\Delta\omega_1 - (\kappa_c^2 - \omega^2)(\omega^2 - \omega_1^2) + \Delta^2(\omega_1^2 - \omega^2), \\ E_6 &= \omega(-\gamma_1(\Delta^2 + \kappa_c^2 - \omega^2) + 2\kappa_c(\omega^2 - \omega_1^2)), \\ E_7 &= \omega^2(\Delta\Delta_2 - \gamma_1\kappa_c + (\gamma_1 + \kappa_c)\kappa_a + \omega^2) + G_1^2\Delta_2\omega_1, \\ E_8 &= \gamma_1(\Delta\Delta_2 + \kappa_c\kappa_a)\omega + (\gamma_1 + \kappa_c - \kappa_2)\omega^3, \\ E_9 &= (\kappa_c - \kappa_a)\omega\omega_1^2, & F_1 &= E_3E_5 - E_4E_6, \\ F_2 &= E_4E_5 + E_3E_6, & F_3 &= 2J^2(E_7 - E_9), \\ F_4 &= 2J^2(E_8 - E_{10}), & F_5 &= E_1 + F_1 + F_3, \\ F_6 &= F_2 + F_4 - E_2, & D_3 &= \frac{D_2}{\omega}, \end{aligned} \quad (\text{S59})$$

and the rest parameters are given by,

$$\begin{aligned}
H_1 &= 2G_2^2 [J^2 \Delta_2 - \Delta(\Delta_2^2 + \kappa_a^2 - \omega^2)], \\
H_2 &= -4G_2^2 \Delta \kappa_a \omega, \quad H_3 = (\omega^2 - \omega_1^2) \omega_2, \\
H_5 &= H_1 H_3 - H_2 H_4, \quad H_6 = H_2 H_3 + H_1 H_4, \\
L_2 &= F_5 H_6 - F_6 H_5, \quad L_3 = \frac{L_2}{\omega}, \quad H_4 = \gamma_1 \omega \omega_2.
\end{aligned} \tag{S60}$$

We note that the parameter  $S_{\text{rp},j}$  in Eq. (S50) denotes the radiation-pressure noise spectra of the  $j$ th vibration defined as:

$$S_{\text{rp},1}(\omega) = \frac{G_1^2 W_1(\omega) |Z_1(\omega)|^2}{|N_2(\omega)|^2}, \tag{S61a}$$

$$S_{\text{rp},2}(\omega) = \frac{G_2^2 W_1(\omega) |Z_2(\omega)|^2}{|M_2(\omega)|^2}, \tag{S61b}$$

while the parameter  $S_{\text{th},j}$  in Eq. (S50) represents the thermal noise spectrum of the  $j$ th mechanical motion which is defined as,

$$S_{\text{th},1}(\omega) = \frac{\gamma_1 \omega}{\omega_1} \coth\left(\frac{\omega}{2k_B T_1}\right) \approx \gamma_1 (2\bar{n}_{\text{th},1} + 1), \tag{S62a}$$

$$S_{\text{th},2}(\omega) = \frac{\gamma_2 \omega}{\omega_2} \coth\left(\frac{\omega}{2k_B T_2}\right) \approx \gamma_2 (2\bar{n}_{\text{th},2} + 1), \tag{S62b}$$

and the parameter  $S_{\text{EP},j}$  in Eq. (S50) is the EP-induced noise spectra of the  $j$ th mechanical vibration, which is defined as,

$$S_{\text{EP},1}(\omega) = \frac{N_1(\omega)}{|N_2(\omega)|^2}, \tag{S63a}$$

$$S_{\text{EP},2}(\omega) = \frac{M_1(\omega)}{|M_2(\omega)|^2}, \tag{S63b}$$

where

$$\begin{aligned}
Z_1 &= i\gamma_2 \omega + \omega^2 - \omega_2^2, \quad Z_2 = i\gamma_1 \omega + \omega^2 - \omega_1^2, \quad K_1 = \Delta^2 + (\kappa_c + i\omega)^2, \\
K_2 &= \Delta_2^2 + (\kappa_a - i\omega)^2, \quad T_1 = \Delta \Delta_2 + (-i\kappa_c + \omega)(i\kappa_a + \omega), \\
N_2 &= J^4 (i\gamma_2 \omega - \omega^2 + \omega_2^2) + K_2 (\omega (i\gamma_2 - \omega) K_1 - 2G_2^2 \Delta \omega_2 + K_1 \omega_2^2) \\
&\quad + 2J^2 (\omega (-i\gamma_2 + \omega) T_1 + G_2^2 \Delta_2 \omega_2 - T_1 \omega_2^2), \\
M_2 &= J^4 (i\gamma_1 \omega - \omega^2 + \omega_1^2) + K_2 (\omega (i\gamma_1 - \omega) K_1 - 2G_1^2 \Delta \omega_1 + K_1 \omega_1^2) \\
&\quad + 2J^2 (\omega (-i\gamma_1 + \omega) T_1 + G_1^2 \Delta_2 \omega_1 - T_1 \omega_1^2), \\
W_1 &= (2(J^6 \kappa_a + J^4 (f_1 + (\kappa_c - 2\kappa_a) \omega^2)) + J^2 (f_2 (\Delta_2^2 + \kappa_a^2) + (2\Delta_2 (\Delta + \Delta_2) \kappa_c \\
&\quad + h_1 \kappa_a - 2\kappa_c \kappa_a^2 + \kappa_a^3) \omega^2 + (\kappa_a - 2\kappa_c) \omega^4) + \kappa_c (\Delta^2 + \kappa_c^2 + \omega^2) \\
&\quad \times (\Delta_2^4 + 2\Delta_2^2 (\kappa_a - \omega) (\kappa_a + \omega) + \kappa_a^2 + \omega^2)^2), \\
h_1 &= \Delta^2 + 4\Delta \Delta_2 + \Delta_2^2 - \kappa_c^2, \quad f_1 = -2\Delta \Delta_2 \kappa_a + \Delta_2^2 \kappa_c - \kappa_c \kappa_a, \\
f_2 &= -2\Delta \Delta_2 \kappa_c + \Delta^2 \kappa_a - \kappa_c^2 \kappa_a, \quad N_1 = 4\omega_2^2 G_1^2 G_2^2 |Y|^2, \\
M_1 &= 4\omega_1^2 G_1^2 G_2^2 |Y|^2, \quad Y = J^2 \Delta_2 - \Delta (\Delta_2^2 + (\kappa_a + i\omega)^2),
\end{aligned} \tag{S64}$$

We should note that in Eq. (S62), we have considered the high-temperature limit  $k_B T_j \gg \hbar \omega_j$ . Here we consider the case of  $N = 2$  and  $\kappa_{c(a)} = \kappa_0$ , and then, the *net refrigeration rate* of the  $j$ th mechanical resonator is derived as:

$$\gamma_{j,C} = 4G_j^2 [1 + \chi_j(J, \Delta)] / \kappa_0, \tag{S65}$$

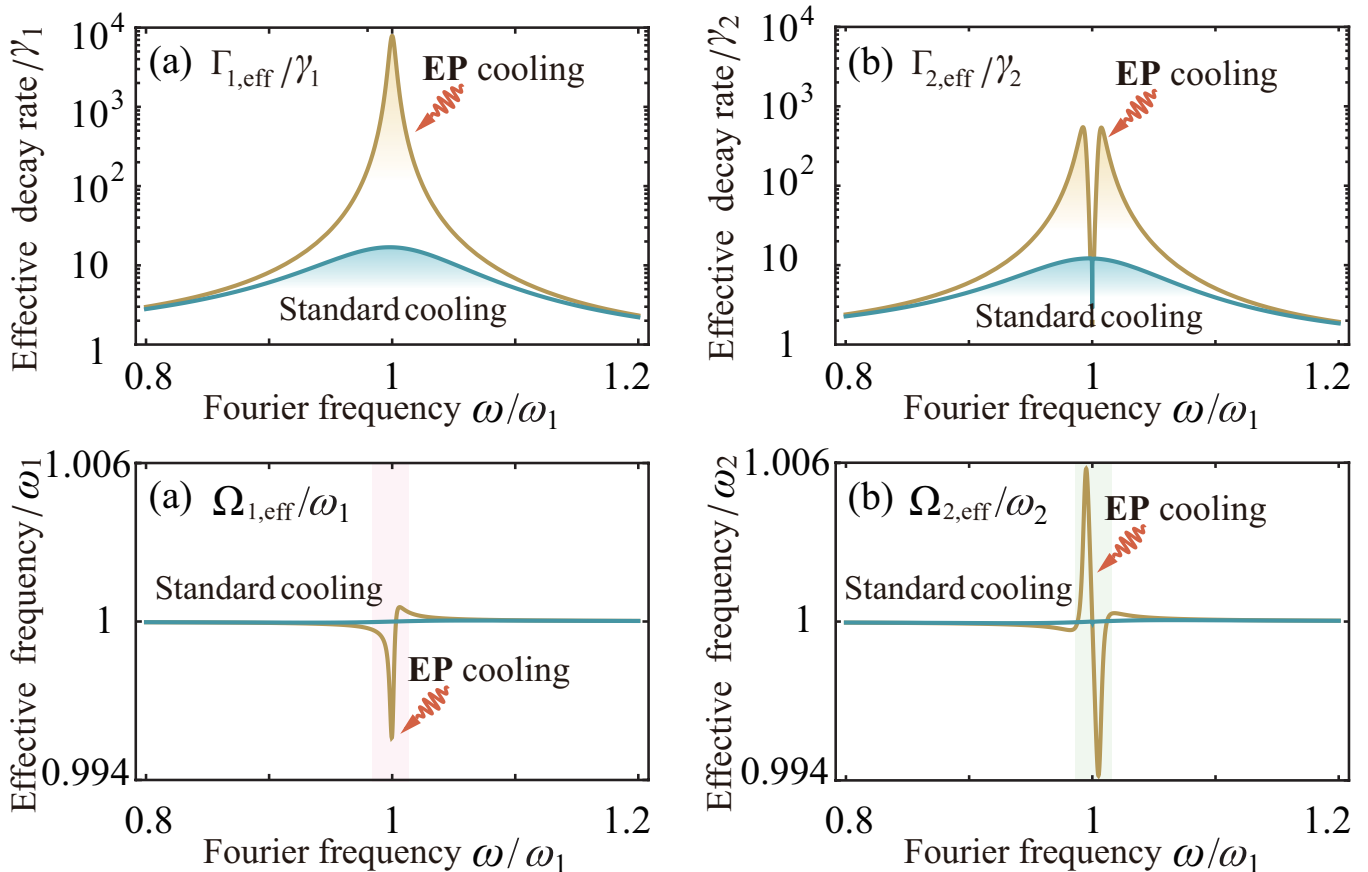


FIG. S2: Effective mechanical decay rates (a)  $\Gamma_{1,\text{eff}}$  [based on Eq. (S52)] of the first mechanical resonator and (b)  $\Gamma_{2,\text{eff}}$  of the second mechanical resonator versus the Fourier frequency  $\omega$  for the cases of the standard cooling (blue curves) and the EP cooling (yellow curves). Effective mechanical resonance frequency (c)  $\Omega_{1,\text{eff}}$  [based on Eq. (S53)] and (d)  $\Omega_{2,\text{eff}}$  versus  $\omega$  in the standard-cooling (blue curves) and the EP-cooling (yellow curves) cases. Other parameters are:  $\omega_1/(2\pi) = 20$  MHz,  $\omega_2/\omega_1 = 0.7$ ,  $\gamma_j/\omega_1 = 10^{-5}$ ,  $\kappa_c/\omega_1 = 1/(5\pi)$ ,  $G_j/\kappa_c = 0.05$ ,  $J/\kappa_c = 0.999$ , and  $\Delta = \omega_1$ .

where  $\chi_j(J, \Delta) = \Lambda_j/\Xi_j$  is the cooling-enhancement factor induced by the EP effect. The parameters  $\Lambda_j$  and  $\Xi_j$  are, respectively, described by:

$$\begin{aligned} \Lambda_j = & \omega_j \Delta [(\Delta^2(\Delta + 2\kappa_{0-}) + \kappa_{0+}^2)[\kappa_0(\gamma_m^2 \omega^2 + \omega_i'^2) + G^2 \gamma_m \Delta \omega_2] \kappa_0 + \Delta \omega_j J^2 \kappa_0 [2(-\kappa_0 \Delta_+ (\gamma_m^2 \omega^2 + \omega_i'^2) \\ & - G^2 \gamma_m \Delta \Delta_- \omega_i) + J^2(\kappa_0(\gamma_m^2 \omega^2 + \omega_i'^2) + G^2 \gamma_m \Delta \omega_i)] - \omega^2 [\gamma_m (J^2 (J^2 - 2\Delta_+) + \kappa_- \kappa_+) + 4G^2 \Delta \kappa_0 \omega_i]^2 \\ & - [\kappa_- \kappa_+ (\omega_i^2 - \omega^2) - 2G^2 \Delta \Delta_- \omega_i + J^2 (2(G^2 \Delta \omega_i + \Delta^2 \omega_i' + \kappa_{0+} \omega_i') - J^2 \omega_i')]^2], \end{aligned} \quad (\text{S66a})$$

$$\begin{aligned} \Xi_j = & \omega^2 [\gamma_m (J^2 (J^2 - 2\Delta_+) + \kappa_- \kappa_+) + 4G^2 \Delta \kappa_0 \omega_i]^2 + [\kappa_- \kappa_+ (\omega_i^2 - \omega^2) - 2G^2 \Delta \Delta_- \omega_i \\ & + J^2 (2(G^2 \Delta \omega_i + \Delta^2 \omega_i' + \kappa_{0+} \omega_i') - J^2 \omega_i')]^2, \end{aligned} \quad (\text{S66b})$$

with  $\kappa_{\pm} = \kappa_0^2 + (\Delta \pm \omega)^2$ ,  $\Delta_{\pm} = \Delta^2 + \kappa_{0\pm}$ ,  $\kappa_{0\pm} = \kappa_0^2 \pm \omega^2$ , and  $\omega_j' = \omega^2 - \omega_j^2$  for  $i = 3 - j$ .

In the above sections, the effective mechanical damping rate  $\Gamma_{j,\text{eff}}$  and the effective mechanical resonance frequency  $\Omega_{j,\text{eff}}$  of the  $j$ th mechanical vibration are analytically derived [see Eqs. (S52) and (S53)]. In addition, we obtained the numerical results of the final mean thermal excitation numbers in the mechanical vibrations [see Eq. (S30)]. Now, we study how the EP mechanism affects the optomechanical-refrigeration performance by analyzing the dependence of the effective mechanical decay rate  $\Gamma_{j,\text{eff}}$  and the effective mechanical resonance frequency  $\Omega_{j,\text{eff}}$  of the  $j$ th mechanical oscillator on the Fourier frequency  $\omega$ .

In Fig. S2, we show the effective mechanical decay rates  $\Gamma_{1,\text{eff}}$  and  $\Gamma_{2,\text{eff}}$  of the two mechanical vibrations versus the Fourier frequency  $\omega$  for the cases of the standard cooling (blue curves) and the EP cooling (yellow curves). We see that in these two cases, the maximum effective mechanical decay rates  $\Gamma_{j,\text{eff}}$  of the  $j$ th mechanical resonators are located around  $\omega \approx \omega_1$ . In addition, we find that in the EP-cooling case, the maximum value of  $\Gamma_{j,\text{eff}}$  of the  $j$ th

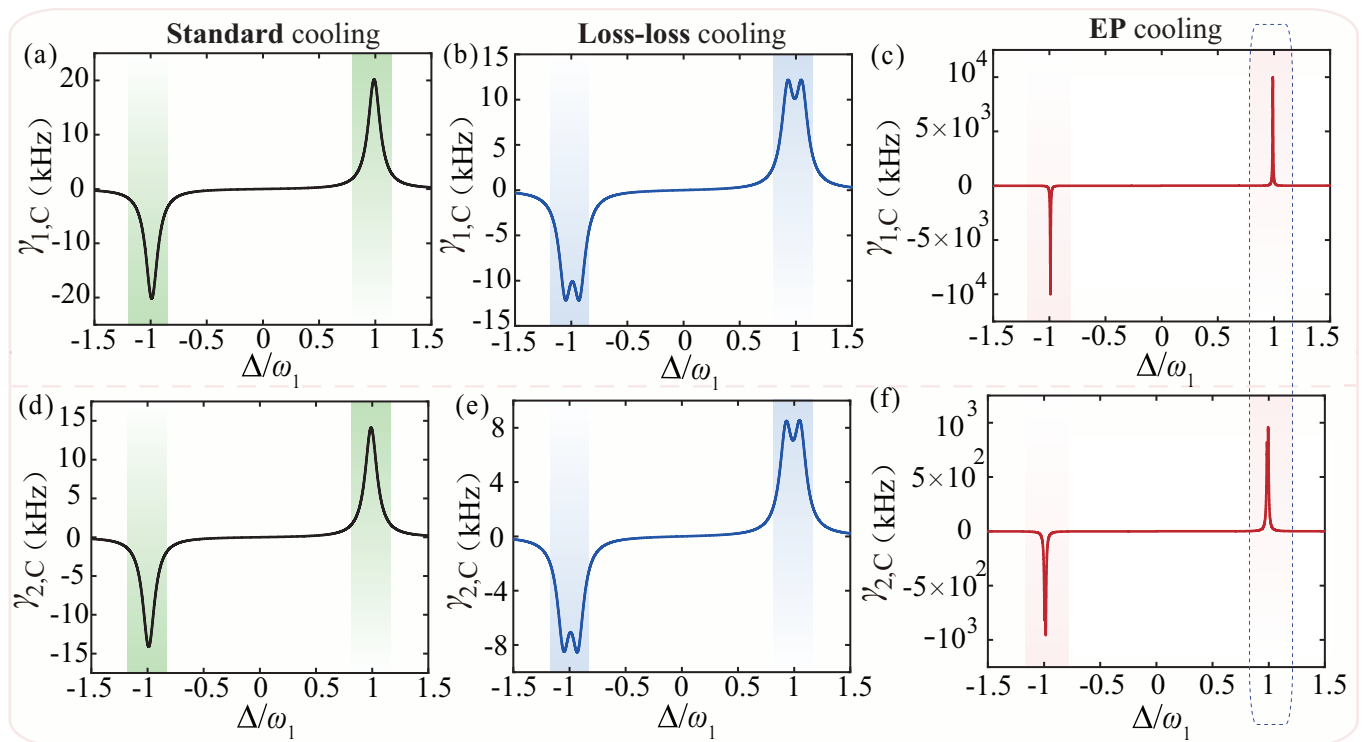


FIG. S3: Net cooling rates (a,b,c)  $\gamma_{1,C}$  [based on Eq. (S54a)] of the first mechanical resonator and (d,e,f)  $\gamma_{2,C}$  [based on Eq. (S54b)] of the second mechanical resonator versus the cavity-field driving detuning  $\Delta$  for the cases of (a,d) the standard cooling (black curves), (b,e) the loss-loss (LL) cooling (blue curves), and (c,f) the EP cooling (red curves). Other parameters are:  $\omega_1/(2\pi) = 20$  MHz,  $\omega_2/\omega_1 = 0.7$ ,  $\gamma_j/\omega_1 = 10^{-5}$ ,  $\kappa_c/\omega_1 = 1/(5\pi)$ ,  $G_j/\kappa_c = 0.05$ ,  $\omega/\omega_1 = 0.99$ , and  $J/\kappa_c = 0.999$ .

mechanical resonator near  $\Delta = \omega_1$  is much larger than that in the standard-cooling cases [see Figs. S2(a,b)]. Note that  $\Gamma_{2,\text{eff}}$  splits into two peaks of the same height near  $\omega = \omega_1$  [see Fig. S2(b)]. Physically, the effective mechanical decay rates  $\Gamma_{j,\text{eff}}$  can be greatly increased by employing the EP mechanism, which leads to a giant enhancement for the cooling performance and its limit. Specifically, Figs. S2 (a,b) show that in the EP-cooling case, the effective mechanical decay rates  $\Gamma_{j,\text{eff}}$  close the EP are dramatically amplified by at least *three orders of magnitude* compared with the cases without the EP, and that in these two cases, the maximum value of  $\Gamma_{1,\text{eff}}$  is always much larger than that of  $\Gamma_{2,\text{eff}}$ .

Furthermore, the effect of the EP-cooling mechanism on the effective mechanical resonance frequency  $\Omega_{j,\text{eff}}$  of the  $j$ th mechanical resonator is studied in detail. Specifically, we plot  $\Omega_{j,\text{eff}}$  as a function of the Fourier frequency  $\omega$  in the standard-cooling (blue curves) and EP-cooling (yellow curves) cases, as shown in Figs. S2 (c,d). We see that in the standard-cooling case,  $\Omega_{j,\text{eff}}$  changes slightly near the resonance point  $\omega = \omega_1$ , while it can be significantly changed in the EP-cooling case. Physically, this significant change of the effective mechanical resonance frequency is due to the EP effect.

We have obtained the analytical expressions on the net refrigeration rates  $\gamma_{j,C}$  [see Eqs. (S54)] and the shifts  $\delta\omega_j$  of the mechanical resonance frequencies [see Eqs. (S55)] of the  $j$ th mechanical resonator. Below, we show how the EP mechanism affects the cooling performance by analyzing the dependence of the net refrigeration rates  $\gamma_{j,C}$  and the shifts  $\delta\omega_j$  of the mechanical resonance frequencies on the system parameters.

Specifically, in Fig. S3, the net refrigeration rates  $\gamma_{1,C}$  and  $\gamma_{2,C}$  of the two mechanical vibrations are plotted as a function of the cavity-field driving detuning  $\Delta$  in the three cases when:

(i) only one lossy optical cavity is coupled to the two mechanical motions (i.e., the standard-cooling case, see Figs. S3(a) and S3(d), shown by the black solid curves);

(ii) the loss-loss cavity is linked with the two mechanical resonators (i.e., the loss-loss cooling case, see Figs. S3(b) and S3(e), indicated by the blue solid curves);

and (iii) the gain-loss cavity is connected to the two mechanical resonators (i.e., the EP cooling case, see Figs. S3(c) and S3(f), shown by the red solid curves).

We see from Fig. S3 that in all these three cases, the maximum net refrigeration rates of the mechanical resonators are located around  $\Delta \approx \omega_1$ . For the loss-loss cooling case [see Figs. S3(a) and S3(b)], the optomechanically induced

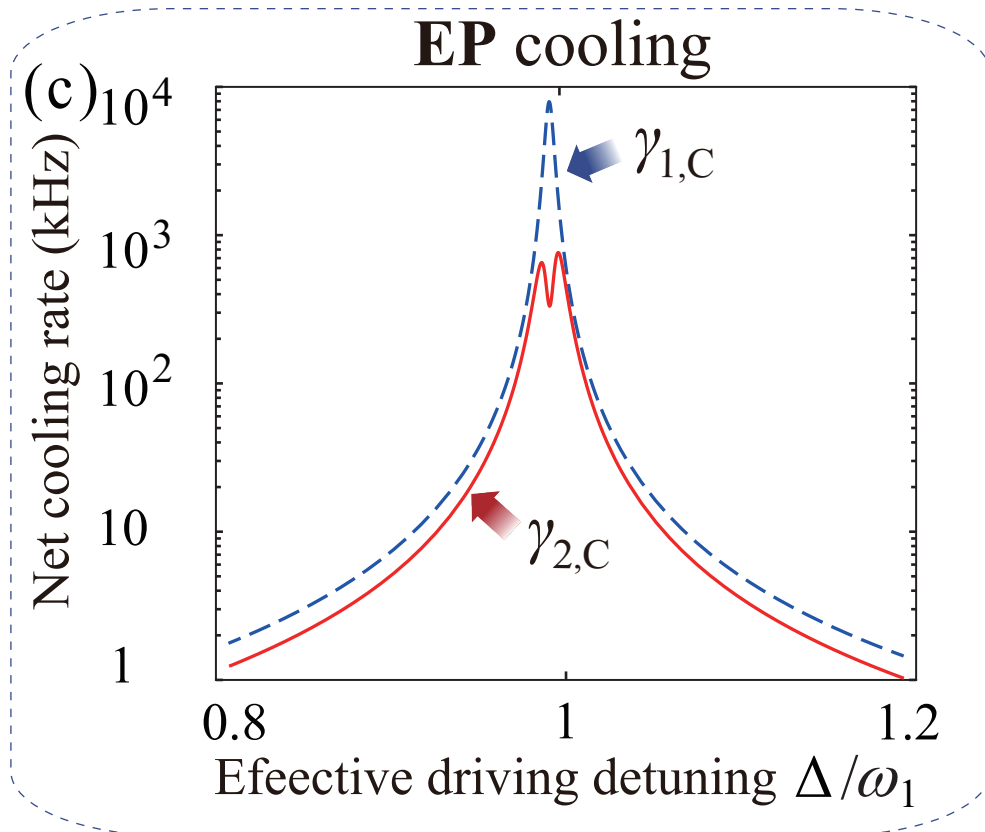


FIG. S4: Net-cooling rates  $\gamma_{1,C}$  (blue dashed curves) and  $\gamma_{2,C}$  (red solid curves) versus the effective driving detuning  $\Delta$  in the EP cooling. Other parameters are the same as those in Fig. S3.

optical net-damping rate  $\gamma_{j,C}$  of the  $j$ th mechanical vibration splits into two peaks of the same height near  $\Delta = \omega_1$ , and the maximum value of the net-refrigeration rates of these mechanical resonators at  $\Delta = \omega_1$  is much smaller than those in both EP- and standard-cooling cases. These findings are quite different from that in the EP-based cooling case [see Figs. S3(c) and S3(f)]. This is because the EP effect greatly increases the net refrigeration rates of the mechanical vibrations, and it corresponds to a giant improvement in the refrigeration performance and its limit. In particular, it is shown in Fig. S3 that in the EP-based cooling case, the net cooling rates at the EP point are giantly amplified by at least *four orders of magnitude* compared with the cases without the EP, and that in these three cases, the maximum net-refrigeration rates of the first mechanical vibration is much larger than that of the second mechanical motion.

To further demonstrate these phenomena, we plot in Fig. S4 the net cooling rates  $\gamma_{1,C}$  (see the blue curves) and  $\gamma_{2,C}$  (red curves) of the two vibrations versus the effective driving detuning  $\Delta$ , when the system operates in the EP cooling. It shows that the maximum net cooling rates of the two mechanical vibrations emerge around  $\Delta \approx \omega_1$ , and the refrigeration rate of the first vibrational mode is larger than that of the second mode. Physically, the first resonator satisfies the resonance condition  $\Delta = \omega_1$  (i.e., the anti-Stokes sideband resonant with the cavity), which is optimal for cooling, while the second vibrational mode is far from that, because its frequency is not equal to that of the first mode. This means that our EP cooling can work for multiple mechanical resonators with the different resonance frequencies.

In addition, we study in detail the dependence of the effective mechanical resonance frequencies of the mechanical resonators on the EP-cooling mechanism. Concretely, in Fig. S5, the shifts of the mechanical resonance frequencies  $\delta\omega_j$  are plotted as a function of the cavity-field driving detuning  $\Delta$  in the three cases:

- (i) the standard-cooling case [see Figs. S5(a) and S5(d), shown by the black solid curves];
- (ii) the loss-loss cooling case [see Figs. S5(b) and S5(e), indicated by the blue solid curves];
- and (iii) the EP-cooling case [see Figs. S5(c) and S5(f), shown by the red solid curves].

It is shown in Figs. S5(a,d) and S5(b,e) that, at the resonance points  $\Delta = \pm\omega_1$ , the resonance frequencies of the mechanical resonators change slightly [ $\delta\omega_j(\pm\omega_j)/\omega_1 \approx \pm 10^{-5}$ ] in the standard-cooling and loss-loss cooling cases, while the resonance frequencies of these resonators in the EP-cooling case are significantly changed [ $\delta\omega_j(\pm\omega_j)/\omega_1 \approx \pm 10^{-2}$ ].

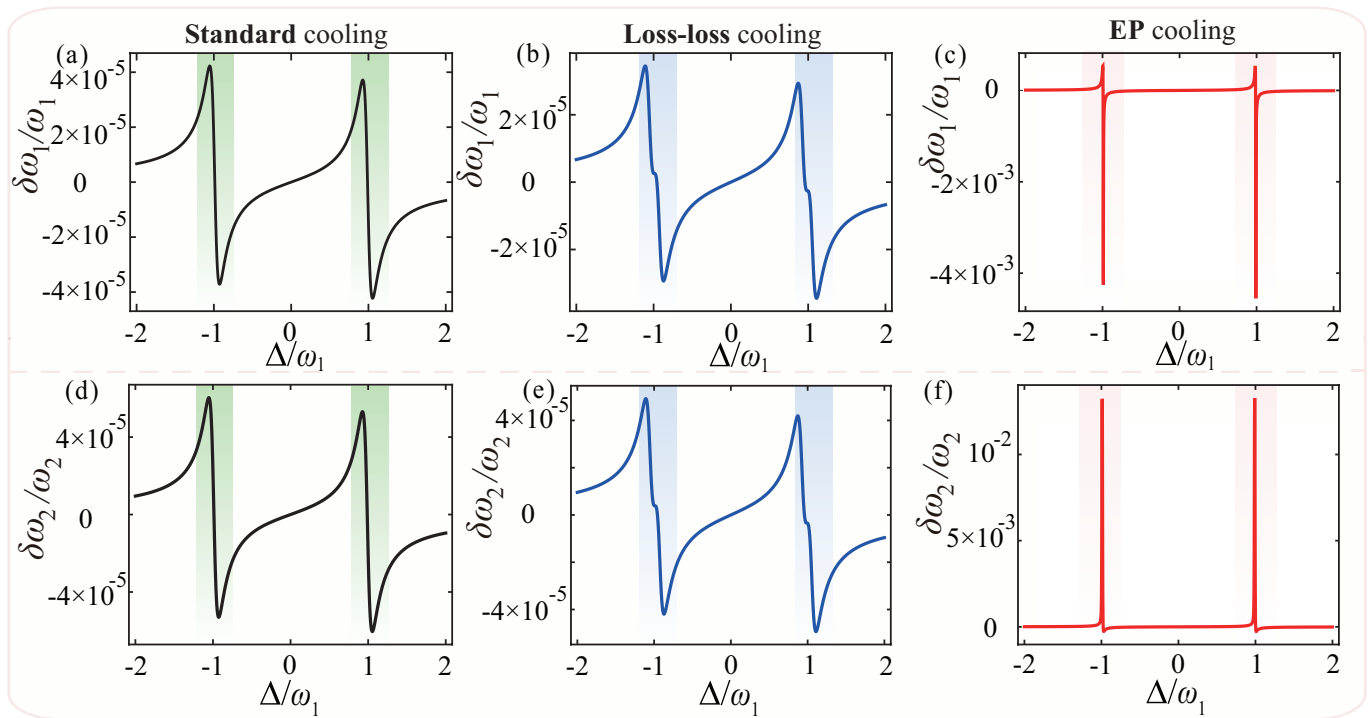


FIG. S5: Mechanical frequency shifts (a,b,c)  $\delta\omega_1$  [based on Eq. (S55a)] of the first mechanical resonator and (d,e,f)  $\delta\omega_2$  [based on Eq. (S55b)] of the second mechanical resonator versus the cavity-field driving detuning  $\Delta$  in (a,d) standard cooling (black curves), (b,e) loss-loss (LL) cooling (blue curves), and (c,f) EP-based cooling (red curves) cases. Other parameters are the same as those in Fig. S3.

Physically, this giant enhancement of the mechanical-resonance frequencies is caused by the EP effect.

In fact, by using the noise spectra [based on Eqs. (S61), (S62), and (S63)] of the two mechanical vibrations, the effective optomechanical refrigeration of these mechanical resonators can be well explained. In Fig. S6, the noise spectra of the two mechanical motions are plotted as a function of the frequency  $\omega$ . Specifically, it is shown that for the first motional mode, at the resonance points  $\omega = \pm\omega_1$ , the contribution from the EP-induced noise  $S_{EP,1}(\omega)$  is much smaller than those from both radiation-pressure noise  $S_{rp,1}(\omega)$  and thermal noise  $S_{th,1}(\omega)$ , as shown in Fig. S6(a).

We can also see that for the second mechanical resonator, at the resonance points  $\omega = \pm\omega_1$ , the contribution from the radiation-pressure noise  $S_{rp,2}(\omega)$  is much larger than that from the thermal noise  $S_{th,2}(\omega)$ , which is approximately equal to that from the EP-induced noise  $S_{EP,2}(\omega)$  [see Fig. S6(b)]. In this way, a giant improvement in the optomechanical-refrigeration performance of these mechanical motions can be realized, because the thermal noise stored in them is significantly suppressed by utilizing the EP-based cooling mechanism. Note that the additional spectral terms, associated to the coupling with the gain cavity, include the EP-induced noise spectral term ( $S_{EP,j}$ ), which is at most comparable to that of usual radiation pressure ( $S_{rp,j}$ ). If starting far away from the quantum regime, a much stronger effect from thermal noise can happen, as shown in Fig. S7.

To further illustrate this point, we plot in Fig. S7 the radiation-pressure noise spectra  $S_{rp,j}$ , thermal noise spectra  $S_{th,j}$ , and EP-induced noise spectra  $S_{EP,j}$  as functions of the initial thermal occupancies  $\bar{n}_{th,j}$ . We see from Fig. S7 and Eqs. (S61-S63) that the thermal-noise spectra  $S_{th,j}$  are governed by the initial thermal phonon numbers  $\bar{n}_{th,j}$ , whereas both the radiation-pressure noise spectra  $S_{rp,j}$  and the EP-induced noise spectra  $S_{EP,j}$  are independent of the initial thermal occupancies  $\bar{n}_{th,j}$ . Close to the classical regime, the contribution from the thermal-noise spectra is enhanced and then, the cooling-improved performance resulted from the EP mechanism deteriorates. This indicates that, far away from the classical regime, the EP mechanism leads to a much better cooling performance for the mechanical resonator; while close to the classical regime, thermal noise is detrimental to refrigeration and tends to cancel the important dependence of the refrigeration enhancement on the EP.

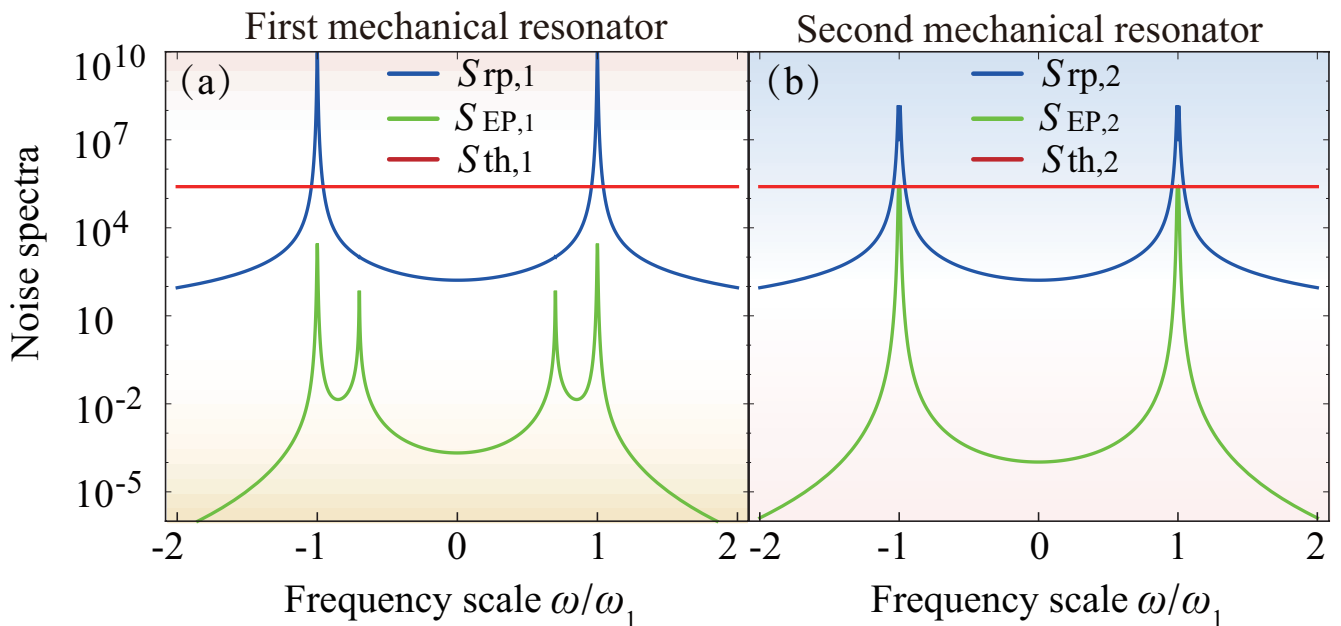


FIG. S6: Radiation-pressure noise spectrum  $S_{rp,j}$  [see Eq. (S61)], the thermal noise spectrum  $S_{th,j}$  [see Eq. (S62)], and the EP-induced noise spectra  $S_{EP,j}$  [see Eq. (S63)] for the  $j$ th mechanical oscillator are plotted as functions of the frequency  $\omega$ . Here we set  $\bar{n}_{th,j} = 100$ , and other parameters are the same as those in Fig. S3.

### C. Analytical expressions of the final average thermal phonon numbers

For the purpose of studying quantum cooling, we need to derive the fluctuation spectra of both momentum and position operators of the mechanical resonators, and then the steady-state mean thermal occupation numbers in these resonators can be obtained, as based on integrating the corresponding fluctuation spectra. Mathematically, the analytical results of the steady-state average phonon numbers in these mechanical resonators can be calculated by using the relation:

$$n_j^f = \frac{1}{2}[\langle \delta q_j^2 \rangle + \langle \delta p_j^2 \rangle - 1], \quad (\text{S67})$$

where the variances  $\delta p_j^2$  and  $\delta q_j^2$  of the momentum and coordinate operators of the  $j$ th mechanical resonator can be obtained by solving Eq. (S44) in the frequency domain and integrating the corresponding fluctuation spectra,

$$\langle \delta q_j^2 \rangle = \frac{1}{2\pi} \int_{-\infty}^{\infty} S_{q_j}(\omega) d\omega, \quad (\text{S68a})$$

$$\langle \delta p_j^2 \rangle = \frac{1}{2\pi} \int_{-\infty}^{\infty} S_{p_j}(\omega) d\omega = \frac{1}{2\pi\omega_j^2} \int_{-\infty}^{\infty} \omega^2 S_{q_j}(\omega) d\omega. \quad (\text{S68b})$$

Now, we present in detail the calculations of the final average thermal phonon numbers in the mechanical resonators. The exact analytical expressions of the steady-state mean thermal phonon numbers in these mechanical resonators can be obtained by calculating the integral in Eq. (S68) for the position and momentum fluctuation spectra. Below, we consider the high-temperature limit  $k_B T_j \gg \hbar\omega_j$ , then it is safe to perform the approximation:

$$\gamma_j \frac{\omega}{\omega_j} \coth\left(\frac{\hbar\omega}{2k_B T_j}\right) \approx \gamma_j (2\bar{n}_{th,j} + 1). \quad (\text{S69})$$

Here the integral kernel used in Eq. (S68) has the form:

$$\frac{g_n(\omega)}{\hbar_n(\omega)\hbar_n(-\omega)}, \quad (\text{S70})$$

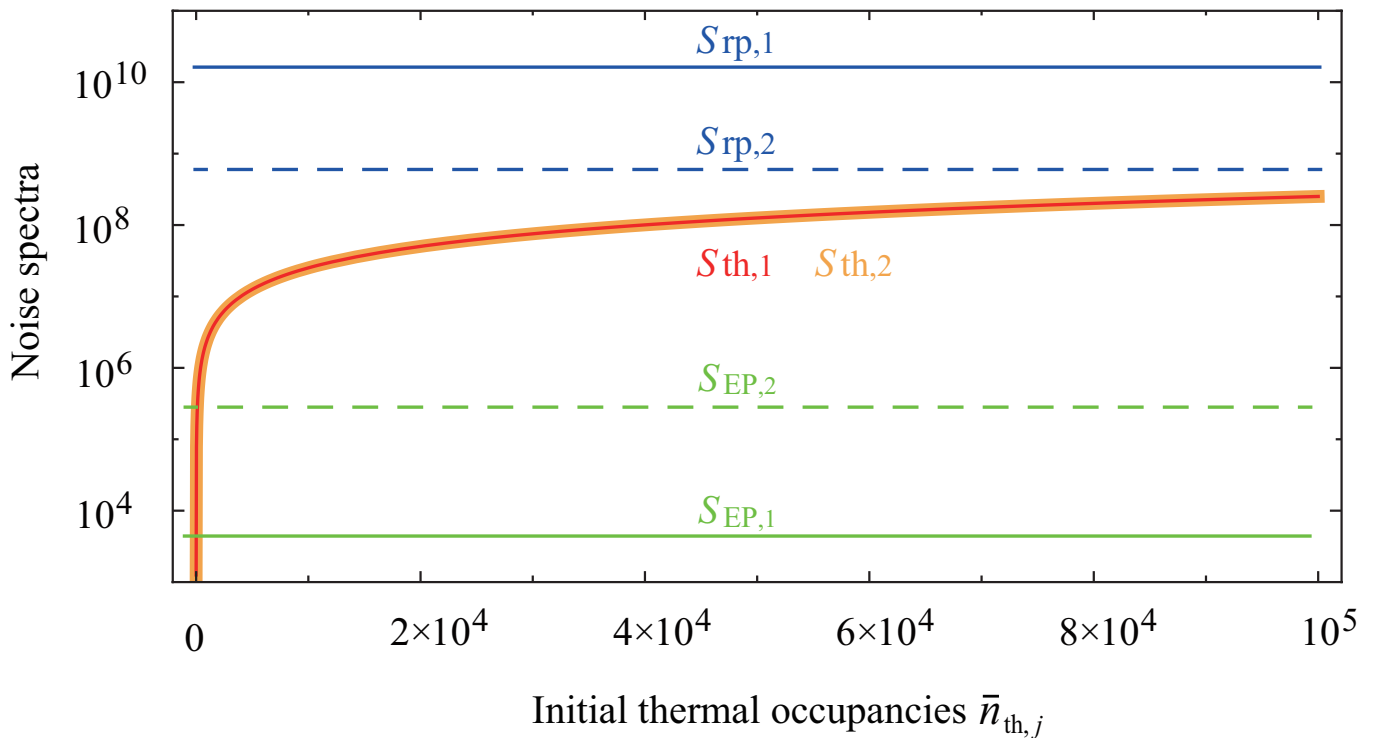


FIG. S7: Radiation-pressure noise spectra  $S_{rp,j}$  [Eq. (S61)], thermal noise spectra  $S_{th,j}$  [Eq. (S62)], and EP-induced noise spectra  $S_{EP,j}$  [Eq. (S63)] as functions of the initial thermal occupancies  $\bar{n}_{th,j}$ . Here we set  $\omega = \omega_1$ , and other parameters are the same as those in Fig. S3.

and this kind of integral can be exactly calculated by the formula [S27]:

$$\int_{-\infty}^{\infty} \frac{g_n(\omega)}{h_n(\omega)h_n(-\omega)} d\omega = \frac{i\pi}{a_0} \frac{M_n}{\mathcal{F}_n}, \quad (\text{S71})$$

where

$$g_n(\omega) = b_0\omega^{2n-2} + b_1\omega^{2n-4} \dots + b_{n-1}, \quad (\text{S72})$$

$$h_n(\omega) = a_0\omega^n + a_1\omega^{n-1} \dots + a_n, \quad (\text{S73})$$

with the parameters  $a_{0,1,2,\dots}$  and  $b_{0,1,2,\dots}$  being the coefficients specified below.

The variables  $\mathcal{F}_n$  and  $M_n$  in Eq. (S71) are, respectively, defined by the following determinants [S27]:

$$\mathcal{F}_n = \begin{vmatrix} a_1 & a_3 & a_5 & \dots & 0 \\ a_0 & a_2 & a_4 & & 0 \\ 0 & a_1 & a_3 & & 0 \\ \vdots & & & \ddots & \\ 0 & 0 & 0 & & a_n \end{vmatrix}, \quad M_n(D_n) = \begin{vmatrix} b_0 & b_1 & b_2 & \dots & b_{n-1} \\ a_0 & a_2 & a_4 & & 0 \\ 0 & a_1 & a_3 & & 0 \\ \vdots & & & \ddots & \\ 0 & 0 & 0 & & a_n \end{vmatrix}. \quad (\text{S74})$$

We can exactly calculate the integral in Eq. (S68) by applying the above formula, and then, the steady-state average thermal phonon numbers in the two mechanical resonators can be obtained as ( $n = 8$  for our four-mode system):

$$n_{s=1,2}^f = \frac{1}{2} \left( \frac{iD_s^{(s)}}{2\mathcal{F}_s} + \frac{iM_s^{(s)}}{2\mathcal{F}_s} - 1 \right), \quad (\text{S75})$$

where  $\mathcal{F}_8$ ,  $D_8^{(s)}$ , and  $M_8^{(s)}$  shown in Eq. (S74) are, respectively, given by:

$$\begin{aligned}
\mathcal{F}_8 = & -a_1^4 a_8^3 + a_0(a_7(-a_3^3 a_6^2 + a_2^2(a_4 a_5 a_6 - a_4^2 a_7 + 2a_2 a_6 a_7) - a_3(a_2 a_5^2 a_6 + a_5(-a_2 a_4 + 3a_0 a_6)a_7 + (a_2^2 - 2a_0 a_4)a_7^2) \\
& + a_0(a_5^3 a_6 - a_4 a_5^2 a_7 + a_2 a_5 a_7^2 - a_0 a_7^3)) + (-a_0 a_5^4 + a_3 a_5^2(a_2 a_5 + 4a_0 a_7) + a_3^3(a_5 a_6 + 2a_4 a_7) - a_3^2(a_4 a_5^2 + 3a_2 a_5 a_7 \\
& + 2a_0 a_7^2))a_8 - a_4^3 a_8^2 + a_1(a_7(a_6(a_5(-a_2 a_3 a_4 + a_2^2 a_5 - 2a_0 a_4 a_5) + a_3(a_2 a_3 + 3a_0 a_5)a_6) + (a_0 a_4(2a_4 a_5 - a_3 a_6) \\
& - a_2^2(a_4 a_5 + 2a_3 a_6) + a_2(a_3 a_4^2 + a_0 a_5 a_6))a_7 + (a_2^3 - 3a_0 a_2 a_4 + 3a_0^2 a_6)a_7^2) + (-a_5(a_5(-a_2 a_3 a_4 + a_2^2 a_5 - 2a_0 a_4 a_5) \\
& + a_3(a_2 a_3 + 3a_0 a_5)a_6) - (-3a_2^2 a_3 a_5 + a_2(2a_3^2 a_4 + a_0 a_5^2) + a_0 a_3(4a_4 a_5 + a_3 a_6))a_7 + a_0(5a_2 a_3 - 4a_0 a_5)a_7^2)a_8 \\
& + a_2^3(a_2 a_3 + 4a_0 a_5)a_8^2 + a_1^3(a_6^3 a_7 - a_6(a_5 a_6 + 3a_4 a_7)a_8 + (2a_4 a_5 + a_3 a_6 + 3a_2 a_7)a_8^2) + a_1^2(a_7(a_6(a_4^2 a_5 - a_3 a_4 a_6 \\
& - 2a_2 a_5 a_6) - (a_4^3 - 3a_2 a_4 a_6 + 3a_0 a_6^2)a_7) + (a_5(-a_4^2 a_5 + a_3 a_4 a_6 + 2a_2 a_5 a_6) + (2a_3 a_4^2 - a_2 a_4 a_5 + a_2 a_3 a_6 \\
& + 5a_0 a_5 a_6)a_7 - 3(a_2^2 - a_0 a_4)a_7^2)a_8 - (a_3^2 a_4 + 3a_2 a_3 a_5 + 2a_0 a_5^2 + 4a_0 a_3 a_7)a_8^2, \tag{S76}
\end{aligned}$$

$$\begin{aligned}
D_8^{(s)} = & \frac{1}{a_8}((a_8(-a_2^3 a_7^3 + a_7(-a_1^2 a_6^3 + a_1(-a_4^2 a_5 a_6 + a_3 a_4 a_6^2 + a_4^3 a_7 + 2a_0 a_6^2 a_7) - a_0(-a_4 a_5^2 a_6 + a_4^2 a_5 a_7 \\
& + a_6(a_3 a_5 a_6 + a_0 a_7^2))) + (a_5(a_1^2 a_6^2 + a_1 a_4(a_4 a_5 - a_3 a_6) + a_0 a_5(-a_4 a_5 + a_3 a_6)) + (a_1 a_4 - a_0 a_5) \\
& (-2a_3 a_4 + 3a_1 a_6)a_7 + a_0(-2a_1 a_4 + a_0 a_5)a_7^2)a_8 + (-a_0 a_3^2 a_5 - a_1^2(2a_4 a_5 + a_3 a_6) + a_1(a_2^2 a_4 + a_0 a_5^2 \\
& + 2a_0 a_3^3 a_7))a_8^2 + a_1^3 a_8^3 + a_2(-a_7(a_2^3 a_6^2 + a_0 a_7(a_5 a_6 - 2a_4 a_7) + a_3 a_4(-a_5 a_6 + a_4 a_7) + a_1 a_6(-2a_5 a_6 \\
& + 3a_4 a_7)) + (a_2^3(a_5 a_6 + 2a_4 a_7) + a_5(-2a_1 a_5 a_6 + a_1 a_4 a_7 + a_0 a_5 a_7) - a_3(a_4 a_5^2 + a_7(a_1 a_6 + 2a_0 a_7)))a_8 \\
& - (a_3^3 - 3a_1 a_3 a_5 + 3a_1^2 a_7)a_8^2) + a_2^2(-a_5^2 a_6 a_7 + a_5^3 a_8 + a_7^2(2a_3 a_6 + 3a_1 a_8) + a_5 a_7(a_4 a_7 - 3a_3 a_8)))b_0^{(s)} \\
& + (a_0 a_8(a_7(a_6(-a_3 a_4 a_5 + a_2^3 a_6 + a_5(a_2 a_5 - a_1 a_6)) + (-a_2 a_4 a_5 + a_1 a_4 a_6 + a_0 a_5 a_6 + a_3(a_4^2 - 2a_2 a_6)a_7 \\
& + (a_2^2 - a_0 a_4)a_7^2) + (a_3 a_4 a_5^2 + a_5^2(a_1 a_6 - a_0 a_7) + a_3 a_7(3a_2 a_5 + a_1 a_6 + a_0 a_7) - a_2^2(a_5 a_6 + 2a_4 a_7) \\
& - a_2(a_5^3 + 2a_1 a_7^2))a_8 + (a_3^3 - 2a_1 a_3 a_5 + a_1^2 a_7)a_8^2))b_1^{(s)} + (a_0 a_8(a_1^2 a_8(-a_6 a_7 + a_5 a_8) + a_1(a_7(a_4 a_5 a_6 \\
& - a_4^2 a_7 + a_6(-a_3 a_6 + a_2 a_7)) + (-a_4 a_5^2 + a_3 a_5 a_6 + 2a_3 a_4 a_7 - a_2 a_5 a_7 + a_0 a_7^2)a_8 - a_2^3 a_8^2) + a_0(-a_5^2 a_6 a_7 \\
& + a_7^2(a_3 a_6 - a_2 a_7) + a_5^3 a_8 + a_5 a_7(a_4 a_7 - 2a_3 a_8)))b_2^{(s)} + (a_0 a_8(a_1 a_7(-a_2 a_5 a_6 + a_2 a_4 a_7 - 2a_0 a_6 a_7) \\
& + a_1(2a_0 a_5 a_7 + a_2(a_5^2 - a_3 a_7))a_8 + a_1^2(a_6^2 a_7 - (a_5 a_6 + a_4 a_7)a_8 + a_3 a_8^2) + a_0(a_0 a_7^3 + a_3(a_5 a_6 a_7 - a_5^2 a_8 \\
& + a_7(-a_4 a_7 + a_3 a_8))))b_3^{(s)} + (-a_0 a_8(a_0 a_7(a_2^3 a_6 - a_2 a_3 a_7 + a_0 a_5 a_7) + a_1 a_7(-a_2 a_3 a_6 + a_2^2 a_7 - a_0(a_5 a_6 \\
& + a_4 a_7)) - a_0 a_3^2 a_5 a_8 + a_1(a_2 a_3 a_5 + a_0(a_5^2 + 2a_3 a_7))a_8 + a_1^3 a_8^2 + a_1^2(a_4 a_6 a_7 - a_4 a_5 a_8 - 2a_2 a_7 a_8)))b_4^{(s)} \\
& + (a_0 a_8(a_1 a_7(-a_2 a_3 a_4 + a_2^2 a_5 - 2a_0 a_4 a_5 + a_0 a_3 a_6 + a_0 a_2 a_7) + a_1 a_3(a_2 a_3 + 2a_0 a_5)a_8 + a_1^3 a_6 a_8 \\
& - a_0(-a_2^3 a_4 a_7 - a_0 a_5^2 a_7 + a_3 a_7(a_2 a_5 + a_0 a_7) + a_3^3 a_8) + a_1^2((a_4^2 - a_2 a_6)a_7 - (a_3 a_4 + a_2 a_5 + a_0 a_7)a_8)))b_5^{(s)} \\
& + (-a_0 a_8(a_0(a_0 a_5^3 - a_3^3 a_6 - a_3 a_5(a_2 a_5 + 2a_0 a_7) + a_2^3(a_4 a_5 + a_2 a_7)) + a_1^3(a_6^2 - a_4 a_8) + a_1^2(a_4^2 a_5 - a_3 a_4 a_6 \\
& - 2a_2 a_5 a_6 + a_2 a_4 a_7 - 2a_0 a_6 a_7 + a_2 a_3 a_8 + a_0 a_5 a_8) + a_1(a_2^2(a_5^2 - a_3 a_7) + a_2(-a_3 a_4 a_5 + a_2^3 a_6 + a_0 a_5 a_7) \\
& + a_0(-2a_4 a_5^2 + 3a_3 a_5 a_6 + a_0 a_7^2 - a_2^2 a_8)))b_6^{(s)} + (a_0(a_1^3(a_6^3 - 2a_4 a_6 a_8 + a_2 a_8^2) + a_1^2(-a_4^3 a_7 - 2a_2^2 a_7 a_8 \\
& + a_2 a_6(-2a_5 a_6 + a_3 a_8) + a_4^2(a_5 a_6 + a_3 a_8) + a_4(-a_3 a_6^2 + 3a_2 a_6 a_7 + 2a_0 a_7 a_8) - a_0(3a_6^2 a_7 - 2a_5 a_6 a_8 \\
& + a_3 a_8^2)) - a_0(a_0(-a_5^3 a_6 + a_4 a_5^2 a_7 - a_2 a_5 a_7^2 + a_0 a_7^3) + a_3^3(a_6^2 - a_4 a_8) + a_3^2(-a_4 a_5 a_6 + a_4^2 a_7 - 2a_2 a_6 a_7 \\
& + a_2 a_5 a_8 + a_0 a_7 a_8) + a_3(a_2^2 a_7^2 + a_2 a_5(a_5 a_6 - a_4 a_7) - a_0(-3a_5 a_6 a_7 + 2a_4 a_7^2 + a_5^2 a_8))) + a_1(a_2^3 a_7^2 + a_2^2 \\
& (a_5^2 a_6 - a_4 a_5 a_7 - 2a_3 a_6 a_7 + a_3 a_5 a_8) - a_0(-2a_4^2 a_5 a_7 - 3a_6(a_3 a_5 a_6 + a_0 a_7^2) + (a_2^3 a_6 + 2a_0 a_5 a_7)a_8 + a_4 \\
& (2a_5^2 a_6 + a_3 a_6 a_7 + 2a_3 a_5 a_8)) + a_2(a_0 a_7(a_5 a_6 - 3a_4 a_7) + a_2^3(a_6^2 - a_4 a_8) + a_3(-a_4 a_5 a_6 + a_4^2 a_7 \\
& + 3a_0 a_7 a_8)))b_7^{(s)}, \tag{S77}
\end{aligned}$$

$$\begin{aligned}
M_8^{(s)} = & \frac{1}{\omega_s^2} \frac{1}{a_8} ((a_8(-a_2^3 a_7^3 + a_7(-a_1^2 a_6^3 + a_1(-a_4^2 a_5 a_6 + a_3 a_4 a_6^2 + a_4^3 a_7 + 2a_0 a_6^2 a_7) - a_0(-a_4 a_5^2 a_6 + a_4^2 a_5 a_7 + a_6 \\
& (a_3 a_5 a_6 + a_0 a_7^2))) + (a_5(a_1^2 a_6^2 + a_1 a_4(a_4 a_5 - a_3 a_6) + a_0 a_5(-a_4 a_5 + a_3 a_6)) + (a_1 a_4 - a_0 a_5)(-2a_3 a_4 \\
& + 3a_1 a_6) a_7 + a_0(-2a_1 a_4 + a_0 a_5) a_7^2) a_8 + (-a_0 a_3^2 a_5 - a_1^2(2a_4 a_5 + a_3 a_6) + a_1(a_3^2 a_4 + a_0 a_5^2 + 2a_0 a_3 a_7)) a_8^2 \\
& + a_3^3 a_8^3 + a_2(-a_7(a_3^2 a_6^2 + a_0 a_7(a_5 a_6 - 2a_4 a_7) + a_3 a_4(-a_5 a_6 + a_4 a_7) + a_1 a_6(-2a_5 a_6 + 3a_4 a_7)) + (a_3^2 \\
& (a_5 a_6 + 2a_4 a_7) + a_5(-2a_1 a_5 a_6 + a_1 a_4 a_7 + a_0 a_5 a_7) - a_3(a_4 a_5^2 + a_7(a_1 a_6 + 2a_0 a_7))) a_8 - (a_3^3 - 3a_1 a_3 a_5 \\
& + 3a_1^2 a_7) a_8^2) + a_2^2(-a_5^2 a_6 a_7 + a_5^3 a_8 + a_7^2(2a_3 a_6 + 3a_1 a_8) + a_5 a_7(a_4 a_7 - 3a_3 a_8))) b_0^{(s)} + (a_0 a_8(a_7(a_6 \\
& (-a_3 a_4 a_5 + a_3^2 a_6 + a_5(a_2 a_5 - a_1 a_6)) + (-a_2 a_4 a_5 + a_1 a_4 a_6 + a_0 a_5 a_6 + a_3(a_4^2 - 2a_2 a_6)) a_7 + (a_2^2 - a_0 a_4) \\
& a_7^2) + (a_3 a_4 a_5^2 + a_5^2(a_1 a_6 - a_0 a_7) + a_3 a_7(3a_2 a_5 + a_1 a_6 + a_0 a_7) - a_3^2(a_5 a_6 + 2a_4 a_7) - a_2(a_5^3 + 2a_1 a_7^2)) a_8 \\
& + (a_3^3 - 2a_1 a_3 a_5 + a_1^2 a_7) a_8^2) b_1^{(s)} + (a_0 a_8(a_1^2 a_8(-a_6 a_7 + a_5 a_8) + a_1(a_7(a_4 a_5 a_6 - a_4^2 a_7 + a_6(-a_3 a_6 + a_2 a_7)) \\
& + (-a_4 a_5^2 + a_3 a_5 a_6 + 2a_3 a_4 a_7 - a_2 a_5 a_7 + a_0 a_7^2) a_8 - a_3^2 a_8^2) + a_0(-a_5^2 a_6 a_7 + a_7^2(a_3 a_6 - a_2 a_7) + a_5^3 a_8 \\
& + a_5 a_7(a_4 a_7 - 2a_3 a_8))) b_2^{(s)} + (a_0 a_8(a_1 a_7(-a_2 a_5 a_6 + a_2 a_4 a_7 - 2a_0 a_6 a_7) + a_1(2a_0 a_5 a_7 + a_2(a_5^2 - a_3 a_7)) a_8 \\
& + a_1^2(a_6^2 a_7 - (a_5 a_6 + a_4 a_7) a_8 + a_3 a_8^2) + a_0(a_0 a_7^3 + a_3(a_5 a_6 a_7 - a_5^2 a_8 + a_7(-a_4 a_7 + a_3 a_8)))) b_3^{(s)} \\
& + (-a_0 a_8(a_0 a_7(a_3^2 a_6 - a_2 a_3 a_7 + a_0 a_5 a_7) + a_1 a_7(-a_2 a_3 a_6 + a_2^2 a_7 - a_0(a_5 a_6 + a_4 a_7)) - a_0 a_3^2 a_5 a_8 \\
& + a_1(a_2 a_3 a_5 + a_0(a_5^2 + 2a_3 a_7)) a_8 + a_1^3 a_8^2 + a_1^2(a_4 a_6 a_7 - a_4 a_5 a_8 - 2a_2 a_7 a_8)) b_4^{(s)} + (a_0 a_8(a_1 a_7(-a_2 a_3 a_4 \\
& + a_2^2 a_5 - 2a_0 a_4 a_5 + a_0 a_3 a_6 + a_0 a_2 a_7) + a_1 a_3(a_2 a_3 + 2a_0 a_5) a_8 + a_1^3 a_6 a_8 - a_0(-a_3^2 a_4 a_7 - a_0 a_5^2 a_7 \\
& + a_3 a_7(a_2 a_5 + a_0 a_7) + a_3^3 a_8) + a_1^2((a_4^2 - a_2 a_6) a_7 - (a_3 a_4 + a_2 a_5 + a_0 a_7) a_8)) b_5^{(s)} + (-a_0 a_8(a_0(a_0 a_5^3 \\
& - a_3^3 a_6 - a_3 a_5(a_2 a_5 + 2a_0 a_7) + a_3^2(a_4 a_5 + a_2 a_7)) + a_1^3(a_6^2 - a_4 a_8) + a_1^2(a_4^2 a_5 - a_3 a_4 a_6 - 2a_2 a_5 a_6 \\
& + a_2 a_4 a_7 - 2a_0 a_6 a_7 + a_2 a_3 a_8 + a_0 a_5 a_8) + a_1(a_2^2(a_5^2 - a_3 a_7) + a_2(-a_3 a_4 a_5 + a_3^2 a_6 + a_0 a_5 a_7) \\
& + a_0(-2a_4 a_5^2 + 3a_3 a_5 a_6 + a_0 a_7^2 - a_3^2 a_8))) b_6^{(s)} + (a_0(a_3^3(a_6^3 - 2a_4 a_6 a_8 + a_2 a_8^2) + a_1^2(-a_4^3 a_7 - 2a_2^2 a_7 a_8 \\
& + a_2 a_6(-2a_5 a_6 + a_3 a_8) + a_4^2(a_5 a_6 + a_3 a_8) + a_4(-a_3 a_6^2 + 3a_2 a_6 a_7 + 2a_0 a_7 a_8) - a_0(3a_6^2 a_7 - 2a_5 a_6 a_8 \\
& + a_3 a_8^2)) - a_0(a_0(-a_5^3 a_6 + a_4 a_5^2 a_7 - a_2 a_5 a_7^2 + a_0 a_7^3) + a_3^3(a_6^2 - a_4 a_8) + a_3^2(-a_4 a_5 a_6 + a_4^2 a_7 \\
& - 2a_2 a_6 a_7 + a_2 a_5 a_8 + a_0 a_7 a_8) + a_3(a_2^2 a_7^2 + a_2 a_5(a_5 a_6 - a_4 a_7) - a_0(-3a_5 a_6 a_7 + 2a_4 a_7^2 + a_5^2 a_8))) \\
& + a_1(a_2^3 a_7^2 + a_2^2(a_5^2 a_6 - a_4 a_5 a_7 - 2a_3 a_6 a_7 + a_3 a_5 a_8) - a_0(-2a_4^2 a_5 a_7 - 3a_6(a_3 a_5 a_6 + a_0 a_7^2) + (a_3^2 a_6 \\
& + 2a_0 a_5 a_7) a_8 + a_4(2a_5^2 a_6 + a_3 a_6 a_7 + 2a_3 a_5 a_8)) + a_2(a_0 a_7(a_5 a_6 - 3a_4 a_7) + a_3^2(a_6^2 - a_4 a_8) \\
& + a_3(-a_4 a_5 a_6 + a_4^2 a_7 + 3a_0 a_7 a_8)))) b_7^{(s)}), \tag{S78}
\end{aligned}$$

with  $a_{0,1,2,\dots}$  and  $b_{0,1,2,\dots}$  being coefficients, which are defined as:

$$\begin{aligned}
a_0 &= -1, \\
a_1 &= i(\gamma_1 + \gamma_2 + 2\kappa_c - 2\kappa_a), \\
a_2 &= 2J^2 + \gamma_1 \gamma_2 + \Delta^2 + \Delta_2^2 + 2\gamma_1 \kappa_c + \kappa_c^2 - 2(\gamma_1 + \gamma_2 + 2\kappa_c) \kappa_a + \kappa_a^2 + \omega_1^2 + \omega_2^2, \\
a_3 &= -i(\gamma_2 \Delta^2 + \gamma_2 \Delta_2^2 + 2\Delta_2^2 \kappa_c + \gamma_2 \kappa_c^2 + 2J^2(\gamma_1 + \gamma_2 + \kappa_c - \kappa_a) - 2\Delta^2 \kappa_a - 4\gamma_2 \kappa_c \kappa_a - 2\kappa_c^2 \kappa_a + \gamma_2 \kappa_a^2 + 2\kappa_c \kappa_a^2 \\
&+ \gamma_2 \omega_1^2 + 2\kappa_c \omega_1^2 - 2\kappa_a \omega_1^2 + 2(\kappa_c - \kappa_a) \omega_2^2 + \gamma_1(\Delta^2 + \Delta_2^2 + \kappa_c(2\gamma_2 + \kappa_c) - 2(\gamma_2 + 2\kappa_c) \kappa_a + \kappa_a^2 + \omega_2^2)), \\
a_4 &= -J^4 - \Delta^2 \Delta_2^2 - 2\gamma_2 \Delta_2^2 \kappa_c - \Delta_2^2 \kappa_c^2 + 2\gamma_2 \Delta^2 \kappa_a + 2\gamma_2 \kappa_c^2 \kappa_a - \Delta^2 \kappa_a^2 - 2\gamma_2 \kappa_c \kappa_a^2 - \kappa_c^2 \kappa_a^2 + 2G_1^2 \Delta \omega_1 - \Delta^2 \omega_1^2 \\
&- \Delta_2^2 \omega_1^2 - 2\gamma_2 \kappa_c \omega_1^2 - \kappa_c^2 \omega_1^2 + 2\gamma_2 \kappa_a \omega_1^2 + 4\kappa_c \kappa_a \omega_1^2 - \kappa_a^2 \omega_1^2 + 2G_2^2 \Delta \omega_2 - (\Delta^2 + \Delta_2^2 + \kappa_c^2 - 4\kappa_c \kappa_a + \kappa_a^2 \\
&+ \omega_1^2) \omega_2^2 - 2J^2(\gamma_1 \gamma_2 - \Delta + \Delta_2 + \omega_1 \kappa_c + \omega_2 \kappa_c - (\omega_1 + \omega_2 + \kappa_c) \kappa_a + \omega_1^2 + \omega_2^2) - \omega_1(-2\Delta^2 \kappa_a + \omega_2(\Delta^2 \\
&+ \Delta_2^2 + \kappa_c^2 - 4\kappa_c \kappa_a + \kappa_a^2) + 2\kappa_c(\Delta_2^2 + \kappa_a(-\kappa_c + \kappa_a)) + 2(\kappa_c - \kappa_a) \omega_2^2), \tag{S79}
\end{aligned}$$

$$\begin{aligned}
a_5 &= -i(-J^4(\gamma_1 + \gamma_2 - \gamma_2\Delta^2\Delta_2^2 - \gamma_2\Delta_2^2\kappa_c^2 - \gamma_2\Delta^2\kappa_a^2 - \gamma_2\kappa_c^2\kappa_a^2 + 2G_1^2\Delta\omega_2\omega_1 - 4G_1^2\Delta\kappa_a\omega_1 - \omega_2\Delta^2\omega_1^2 - \omega_2\Delta_2^2\omega_1^2 \\
&\quad - 2\Delta_2^2\kappa_c\omega_1^2 - \gamma_2\kappa_c^2\omega_1^2 + 2\Delta^2\kappa_a\omega_1^2 + 4\gamma_2\kappa_c\kappa_a\omega_1^2 + 2\kappa_c^2\kappa_a\omega_1^2 - \gamma_2\kappa_a^2\omega_1^2 - 2\kappa_c\kappa_a^2\omega_1^2 - 4G_2^2\Delta\kappa_a\omega_2 + 2(-\Delta_2^2\kappa_c \\
&\quad + \Delta^2\kappa_a + (\kappa_c - \kappa_a(\kappa_c\kappa_a - \omega_1^2))\omega_2^2 + \gamma_1(-\Delta_2^2(\Delta^2 + \kappa_c(2\Delta_2 + \kappa_c)) + 2\gamma_2(\Delta^2 + \kappa_c^2)\kappa_a - (\Delta^2 + \kappa_c(2\gamma_2 + \kappa_c))\kappa_a^2 \\
&\quad + 2G_2^2\Delta\omega_2 - (\Delta^2 + \Delta_2^2 + \kappa_c^2 - 4\kappa_c\kappa_a + \kappa_a^2)\omega_2^2) + 2J^2(\gamma_2(\Delta\Delta_2 + \kappa_c\kappa_a - \omega_1^2) + \gamma_1(\Delta\Delta_2 - \gamma_2\kappa_c + (\gamma_2 + \kappa_c)\kappa_a \\
&\quad - \omega_2^2) - (\kappa_c - \kappa_a)(\omega_1^2 + \omega_2^2))), \\
a_6 &= \omega_1(-2G_1^2\Delta(\Delta_2^2 - 2\gamma_2\kappa_a + \kappa_a^2) + (\Delta_2^2(\Delta^2 + 2\gamma_2\kappa_c + \kappa_c^2) - 2\gamma_2(\Delta^2 + \kappa_c^2)\kappa_a + (\Delta^2 + 2\gamma_2\kappa_c + \kappa_c^2)\kappa_a^2)\omega_1) - 2G_2^2\Delta \\
&\quad (\Delta_2^2 + \kappa_a^2 + \omega_1^2)\omega_2 + ((\Delta^2 + \kappa_c^2)(\Delta_2^2 + \kappa_a^2) - 2G_2^2\Delta\omega_1 + (\Delta^2 + \Delta_2^2 + \kappa_c^2 - 4\kappa_c\kappa_a + \kappa_a^2)\omega_1^2)\omega_2^2 + J^4(\omega_1\omega_2 + \omega_1^2 \\
&\quad + \omega_2^2) + 2J^2(-\gamma_1\gamma_2(\Delta\Delta_2 + \kappa_c\kappa_a) + \omega_1(G_1^2\Delta_2 - (\Delta\Delta_2 - \omega_2\kappa_c + (\omega_2 + \kappa_c)\kappa_a)\omega_1) + G_2^2\Delta_2\omega_2 + \gamma_1(\kappa_c - \kappa_a)\omega_2^2 \\
&\quad + (-\Delta\Delta_2 - \kappa_c\kappa_a + \omega_1^2)\omega_2^2) + \gamma_1(\gamma_2(\Delta^2 + \kappa_c^2)(\Delta_2^2 + \kappa_a^2) + 2\omega_2(G_2^2\Delta\kappa_a\Delta_2^2\kappa_c\omega_2 - \kappa_a(\Delta^2 + \kappa_c^2 - \kappa_c\kappa_a)\omega_2)), \\
a_7 &= -i(\gamma_2\omega_1(2G_1^2(J^2\Delta_2 - \Delta(\Delta_2^2 + \kappa_a^2)) + (J^4 - 2J^2(\Delta\Delta_2 + \kappa_c\kappa_a))\omega_1 + 2G_2^2(J^2\gamma_1\Delta_2 - \gamma_1\Delta(\Delta_2^2 + \kappa_a^2) + 2\Delta\kappa_a\omega_1^2) \\
&\quad \omega_2 + (\gamma_1(J^4 - 2J^2(\Delta\Delta_2 + \kappa_c\kappa_a) + (\Delta^2 + \kappa_c^2)(\Delta_2^2 + \kappa_a^2)) + 4G_1^2\Delta\kappa_a\omega_1 + 2((J^2 + \Delta_2^2)\kappa_c - (J^2 + \Delta^2 + \kappa_c^2)\kappa_a \\
&\quad + \kappa_c\kappa_a^2)\omega_1^2)\omega_2^2), \\
a_8 &= -\omega_1\omega_2(2G_2^2(J^2\Delta_2 - \Delta(\Delta_2^2 + \kappa_a^2))\omega_1 + (2G_1^2(J^2\Delta_2 - \Delta(\Delta_2^2 + \kappa_a^2)) + (J^4 - 2J^2(\Delta\Delta_2 + \kappa_c\kappa_a) + (\Delta^2 + \kappa_c^2) \\
&\quad (\Delta_2^2 + \kappa_a^2))\omega_1)\omega_2), \tag{S80}
\end{aligned}$$

$$b_0^{(1)} = 0,$$

$$b_1^{(1)} = (1 + 2\bar{n}_1)\gamma_1\omega_1^2,$$

$$b_2^{(1)} = \omega_1^2(2G_1^2\kappa_c + (1 + 2\bar{n}_1)\gamma_1(-4J^2 + \gamma_2^2 - 2(\Delta^2 + \Delta_2^2 - \kappa_c^2 - \kappa_a^2 + \omega_2^2))),$$

$$\begin{aligned}
b_3^{(1)} &= \omega_1^2(6J^4(\gamma_1 + 2\bar{n}_1\gamma_1) + 2G_1^2\kappa_c(\gamma_2^2 + \Delta^2 - 2\Delta_2^2 + \kappa_c^2 + 2\kappa_a^2 - 2\omega_2^2) - 2J^2(G_1^2(2\kappa_c - \kappa_a) + 2(1 + 2\bar{n}_1)\gamma_1(\gamma_2^2 \\
&\quad - \Delta^2 + \Delta\Delta_2 - \Delta_2^2 + \kappa_c^2 + \kappa_c\kappa_a + \kappa_a^2 - 2\omega_2^2)) + (1 + 2\bar{n}_1)\gamma_1(\Delta^4 + \Delta_2^4 - 4\Delta_2^2\kappa_c^2 + \kappa_c^4 + 2\Delta_2^2\kappa_a^2 + 4\kappa_c^2\kappa_a^2 \\
&\quad + \kappa_a^4 + 2\gamma_2^2(-\Delta^2 - \Delta_2^2 + \kappa_c^2 + \kappa_a^2) - 4G_2^2\Delta\omega_2 + 4(\Delta_2^2 - \kappa_c^2 - \kappa_a^2)\omega_2^2 + \omega_2^4 + 2\Delta^2(2\Delta_2^2 + \kappa_c^2 - 2\kappa_a^2 + 2\omega_2^2))),
\end{aligned}$$

$$\begin{aligned}
b_3^{(1)} &= \omega_1^2(6J^4(\gamma_1 + 2\bar{n}_1\gamma_1) + 2G_1^2\kappa_c(\gamma_2^2 + \Delta^2 - 2\Delta_2^2 + \kappa_c^2 + 2\kappa_a^2 - 2\omega_2^2) - 2J^2(G_1^2(2\kappa_c - \kappa_a) + 2(1 + 2\bar{n}_1)\gamma_1(\gamma_2^2 \\
&\quad - \Delta^2 + \Delta\Delta_2 - \Delta_2^2 + \kappa_c^2 + \kappa_c\kappa_a + \kappa_a^2 - 2\omega_2^2)) + (1 + 2\bar{n}_1)\gamma_1(\Delta^4 + \Delta_2^4 - 4\Delta_2^2\kappa_c^2 + \kappa_c^4 + 2\Delta_2^2\kappa_a^2 + 4\kappa_c^2\kappa_a^2 \\
&\quad + \kappa_a^4 + 2\gamma_2^2(-\Delta^2 - \Delta_2^2 + \kappa_c^2 + \kappa_a^2) - 4G_2^2\Delta\omega_2 + 4(\Delta_2^2 - \kappa_c^2 - \kappa_a^2)\omega_2^2 + \omega_2^4 + 2\Delta^2(2\Delta_2^2 + \kappa_c^2 - 2\kappa_a^2 + 2\omega_2^2))), \tag{S81}
\end{aligned}$$

$$\begin{aligned}
b_4^{(1)} &= \omega_1^2(-4J^6(\gamma_1 + 2\bar{n}_1\gamma_1) + 2G_1^2\kappa_c(-2\Delta^2\Delta_2^2 + \Delta_2^4 - 2\Delta_2^2\kappa_c^2 + 2\Delta^2\kappa_a^2 + 2\Delta_2^2\kappa_a^2 + 2\kappa_c^2\kappa_a^2 + \kappa_a^4 + \gamma_2^2(\Delta^2 - 2\Delta_2^2 \\
&\quad + \kappa_c^2 + 2\kappa_a^2) - 2(\Delta^2 - 2\Delta_2^2 + \kappa_c^2 + 2\kappa_a^2)\omega_2^2 + \omega_2^4) + 2J^4(G_1^2(\kappa_c - 2G_1^2\kappa_a) + (1 + 2\bar{n}_1)\gamma_1(3\gamma_2^2 - \Delta^2 + 4\Delta\Delta_2 \\
&\quad - \Delta_2^2 + \kappa_c^2 + 4\kappa_c\kappa_a + \kappa_a^2 - 6\omega_2^2)) + (1 + 2\bar{n}_1)\gamma_1(\gamma_2^2(\Delta^4 + \Delta_2^4 + \kappa_c^4 + 4\kappa_c^2\kappa_a^2 + \kappa_a^4 + 2\Delta^2(2\Delta_2^2 + \kappa_c^2 - 2\kappa_a^2) \\
&\quad + 2\Delta_2^2(-2\kappa_c^2 + \kappa_a^2)) + 8G_2^2\gamma_2\Delta\kappa_c\omega_2 + 2(\kappa_c^2(\Delta_2^4 - \Delta_2^2(\kappa_c^2 - 2\kappa_a^2) + \kappa_a^2(\kappa_c^2 + \kappa_a^2)) + 2G_2^2\Delta^3\omega_2 - (\Delta_2^4 + \kappa_c^4 \\
&\quad + 4\kappa_c^2\kappa_a^2 + \kappa_a^4 + 2\Delta_2^2(-2\kappa_c^2 + \kappa_a^2))\omega_2^2 + (-\Delta_2^2 + \kappa_c^2 + \kappa_a^2)\omega_2^4 + 2G_2^2\Delta\omega_2(2\Delta_2^2 + \kappa_c^2 - 2\kappa_a^2 + \omega_2^2) - \Delta^4(\Delta_2^2 \\
&\quad - \kappa_a^2 + \omega_2^2) - \Delta^2(\Delta_2^4 + \kappa_a^4 - 4\kappa_a^2\omega_2^2 + \omega_2^4 + 2\kappa_c^2(-\kappa_a^2 + \omega_2^2) + 2\Delta_2^2(\kappa_c^2 + \kappa_a^2 + 2\omega_2^2)))) + 2J^2(G_1^2(2\Delta_2^2\kappa_c \\
&\quad + \Delta^2\kappa_a + \Delta_2^2\kappa_a - \kappa_c^2\kappa_a - 2\kappa_c\kappa_a^2 + \kappa_a^3 + \gamma_2^2(-2\kappa_c + \kappa_a) + 2\Delta\Delta_2(\kappa_c + 2\kappa_a) + 4\kappa_c\omega_2^2 - 2\kappa_a\omega_2^2) + 2(1 + 2\bar{n}_1) \\
&\quad \gamma_1(\Delta^3\Delta_2 + \gamma_2^2(\Delta^2 - \Delta\Delta_2 + \Delta_2^2 - \kappa_c^2 - \kappa_c\kappa_a - \kappa_a^2) - \kappa_c(\Delta_2^2(-\kappa_c + \kappa_a) + \kappa_a(\kappa_c^2 + \kappa_c\kappa_a + \kappa_a^2)) - G_2^2\Delta^2\omega_2 \\
&\quad + 2(-\Delta_2^2 + \kappa_c^2 + \kappa_c\kappa_a + \kappa_a^2)\omega_2^2 - \omega_2^4 - \Delta^2(\Delta_2^2 + (\kappa_c - \kappa_a)\kappa_a + 2\omega_2^2) + \Delta(\Delta_2^3 + 2G_2^2\omega_2 + \Delta_2(\kappa_c^2 - 4\kappa_c\kappa_a \\
&\quad + \kappa_a^2 + 2\omega_2^2))))), \tag{S82}
\end{aligned}$$

$$\begin{aligned}
b_5^{(1)} = & \omega_1^2 (J^8 (\gamma_1 + 2\bar{n}_1 \gamma_1) - (1 + 2\bar{n}_1) \gamma_1 (-(\Delta^2 + \kappa_c^2)^2 (\Delta_2^2 + \kappa_a^2)^2 + 2\gamma_2^2 (\Delta_2^2 (\Delta^4 - \Delta_2^2 \kappa_c^2 + \kappa_c^4 + \Delta^2 (\Delta_2^2 + 2\kappa_c^2)) \\
& - (\Delta^4 - 2\Delta^2 \Delta_2^2 + 2(\Delta^2 + \Delta_2^2) \kappa_c^2 + \kappa_c^4) \kappa_a^2 + (\Delta - \kappa_c) (\Delta + \kappa_c) \kappa_a^4) + 16G_2^2 \gamma_2 \Delta \kappa_c (\Delta_2 - \kappa_a) (\Delta_2 + \kappa_a) \omega_2 \\
& + 4G_2^2 \Delta (\Delta_2^2 (2\Delta^2 + \Delta_2^2 + 2\kappa_c^2) - 2(\Delta^2 - \Delta_2^2 + \kappa_c^2) \kappa_a^2 + \kappa_a^4) \omega_2 - 4(G_2^4 \Delta^2 + \Delta_2^2 (\Delta_2^4 - \Delta_2^2 \kappa_c^2 + \kappa_c^4 + \Delta^2 (\Delta_2^2 \\
& + 2\kappa_c^2)) - (\Delta^4 - 2\Delta^2 \Delta_2^2 + 2(\Delta^2 + \Delta_2^2) \kappa_c^2 + \kappa_c^4) \kappa_a^2 + (\Delta - \kappa_c) (\Delta + \kappa_c) \kappa_a^4) \omega_2^2 + 4G_2^2 \Delta (\Delta^2 + 2\Delta_2^2 + \kappa_c^2 \\
& - 2\kappa_a^2) \omega_2^3 - (\Delta^4 + \Delta_2^4 - 4\Delta_2^2 \kappa_c^2 + \kappa_c^4 + 2(\Delta_2^2 + 2\kappa_c^2) \kappa_a^2 + \kappa_a^4 + 2\Delta^2 (2\Delta_2^2 + \kappa_c^2 - 2\kappa_a^2)) \omega_2^4) - 2J^6 (-G_1^2 \kappa_a \\
& + 2(1 + 2\bar{n}_1) \gamma_1 (\gamma_2^2 + \Delta \Delta_2 + \kappa_c \kappa_a - 2\omega_2^2)) + 2J^2 (G_1^2 ((-2\Delta \Delta_2 \kappa_c + \Delta^2 \kappa_a - \kappa_c^2 \kappa_a) (\Delta_2^2 + \kappa_a^2) + \gamma_2^2 (2\Delta_2 (\Delta \\
& + \Delta_2) \kappa_c + (\Delta^2 + 4\Delta \Delta_2 + \Delta_2^2 - \kappa_c^2) \kappa_a - 2\kappa_c \kappa_a^2 + \kappa_a^3) - 2(2\Delta_2 (\Delta + \Delta_2) \kappa_c + (\Delta^2 + 4\Delta \Delta_2 + \Delta_2^2 - \kappa_c^2) \kappa_a \\
& - 2\kappa_c \kappa_a^2 + \kappa_a^3) \omega_2^2 + (-2\kappa_c + \kappa_a) \omega_2^4) + 2(1 + 2\bar{n}_1) \gamma_1 (-(\Delta^2 + \kappa_c^2) (\Delta \Delta_2 + \kappa_c \kappa_a) (\Delta_2^2 + \kappa_a^2) + \gamma_2^2 (\Delta \Delta_2 \\
& (\Delta^2 - \Delta \Delta_2 + \Delta_2^2) + \Delta_2 (\Delta + \Delta_2) \kappa_c^2 - \kappa_c^2 (\Delta^2 + 4\Delta \Delta_2 + \Delta_2^2 + \kappa_c^2) \kappa_a + (\Delta (\Delta + \Delta_2) - \kappa_c^2) \kappa_a^2 - \kappa_c \kappa_a^3) \\
& - 2G_2^2 \gamma_2 ((\Delta - \Delta_2) \kappa_c + (\Delta + \Delta_2) \kappa_a) \omega_2 + G_2^2 (\Delta_2 (3\Delta^2 - 2\Delta \Delta_2 + \Delta_2^2 + \kappa_c^2) - 2(\Delta + 2\Delta_2) \kappa_c \kappa_a + (2\Delta + \Delta_2) \\
& \kappa_a^2) \omega_2 - 2(\Delta \Delta_2 (\Delta^2 - \Delta \Delta_2 + \Delta_2^2) + \Delta_2 (\Delta + \Delta_2) \kappa_c^2 - \kappa_c (\Delta^2 + 4\Delta \Delta_2 + \Delta_2^2 + \kappa_c^2) \kappa_a + (\Delta (\Delta + \Delta_2) - \kappa_c^2) \kappa_a^2 \\
& - \kappa_c \kappa_a^3) \omega_2^2 + G_2^2 (-2\Delta + \Delta_2) \omega_2^3 + (\Delta^2 - \Delta \Delta_2 + \Delta_2^2 - \kappa_c^2 - \kappa_c \kappa_a - \kappa_a^2) \omega_2^4)) + 2G_1^2 (\gamma_2^2 \kappa_c (\Delta_2^2 (-2\Delta^2 \\
& + \Delta_2^2 - 2\kappa_c^2) + 2(\Delta^2 + \Delta_2^2 + \kappa_c^2) \kappa_a^2 + \kappa_a^4) + 2G_2^2 (1 + 2\bar{n}_2) \gamma_2 \Delta^2 \omega_2^2 + \kappa_c ((\Delta^2 + \kappa_c^2) (\Delta_2^2 + \kappa_a^2)^2 - 2(\Delta_2^2 \\
& (-2\Delta^2 + \Delta_2^2 - 2\kappa_c^2) + 2(\Delta^2 + \Delta_2^2 + \kappa_c^2) \kappa_a^2 + \kappa_a^4) \omega_2^2 + (\Delta^2 - 2\Delta_2^2 + \kappa_c^2 + 2\kappa_a^2) \omega_2^4)) + J^4 (2G_1^2 (\Delta_2^2 \kappa_c + \gamma_2^2 \\
& (\kappa_c - 2\kappa_a) - 2\Delta \Delta_2 \kappa_a - \kappa_c \kappa_a^2 - 2(\kappa_c - 2\kappa_a) \omega_2^2) - 2(1 + 2\bar{n}_1) \gamma_1 (\gamma_2^2 (\Delta^2 - 4\Delta \Delta_2 + \Delta_2^2 - \kappa_c^2 - 4\kappa_c \kappa_a - \kappa_a^2) \\
& - \kappa_c^2 (\Delta_2^2 + 3\kappa_a^2) - 4G_2^2 \Delta_2 \omega_2 + 2(-\Delta_2^2 + \kappa_c^2 + 4\kappa_c \kappa_a + \kappa_a^2) \omega_2^2 - 3\omega_2^4 - \Delta^2 (3\Delta_2^2 + \kappa_a^2 + 2\omega_2^2) + \Delta (-4\Delta_2 \kappa_c \kappa_a \\
& + 2G_2^2 \omega_2 + 8\Delta_2 \omega_2^2))),
\end{aligned} \tag{S83}$$

$$\begin{aligned}
b_6^{(1)} = & \omega_1^2 (J^8 (1 + 2\bar{n}_1) \gamma_1 (\gamma_2^2 - 2\omega_2^2) + 2G_1^2 (\gamma_2^2 \kappa_c (\Delta^2 + \kappa_c^2) (\Delta_2^2 + \kappa_a^2)^2 - 4G_2^2 (1 + 2\bar{n}_2) \gamma_2 \Delta^2 (\Delta_2 - \kappa_a) (\Delta_2 + \kappa_a) \omega_2^2 \\
& - 2\kappa_c (\Delta^2 + \kappa_c^2) (\Delta_2^2 + \kappa_a^2)^2 \omega_2^2 + \kappa_c (\Delta_2^2 (-2\Delta^2 + \Delta_2^2 - 2\kappa_c^2) + 2(\Delta^2 + \Delta_2^2 + \kappa_c^2) \kappa_a^2 + \kappa_a^4) \omega_2^4) + (1 + 2\bar{n}_1) \gamma_1 (\gamma_2^2 \\
& (\Delta^2 + \kappa_c^2)^2 (\Delta_2^2 + \kappa_a^2)^2 + 4G_2^2 \Delta (\Delta^2 + \kappa_c (2\gamma_2 + \kappa_c)) (\Delta_2^2 + \kappa_a^2)^2 \omega_2 - 2(4G_2^4 \Delta^2 (\Delta_2 - \kappa_a) (\Delta_2 + \kappa_a) + (\Delta^2 + \kappa_c^2)^2 \\
& (\Delta_2^2 + \kappa_a^2)^2) \omega_2^2 + 4G_2^2 \Delta (\Delta_2^2 (2\Delta^2 + \Delta_2^2 + 2\kappa_c^2) - 2(\Delta^2 - \Delta_2^2 + \kappa_c^2) \kappa_a^2 + \kappa_a^4) \omega_2^3 - 2(\Delta_2^2 (\Delta^4 - \Delta_2^2 \kappa_c^2 + \kappa_c^4 + \Delta^2 \\
& (\Delta_2^2 + 2\kappa_c^2)) - (\Delta^4 - 2\Delta^2 \Delta_2^2 + 2(\Delta^2 + \Delta_2^2) \kappa_c^2 + \kappa_c^4) \kappa_a^2 + (\Delta - \kappa_c) (\Delta + \kappa_c) \kappa_a^4) \omega_2^4) + 2J^4 ((1 + 2\bar{n}_1) \gamma_1 (\gamma_2^2 \\
& (4\Delta \Delta_2 \kappa_c \kappa_a + \Delta^2 (3\Delta_2^2 + \kappa_a^2) + \kappa_c^2 (\Delta_2^2 + 3\kappa_a^2)) + 2G_2^2 (3\Delta \Delta_2 - 2\gamma_2 \Delta_2 \kappa_c + 2\Delta_2 (\gamma_2 + \kappa_c) \kappa_a + \Delta \kappa_a (2\gamma_2 + \kappa_a)) \omega_2 \\
& - 2(4\Delta \Delta_2 \kappa_c \kappa_a + \Delta^2 (3\Delta_2^2 + \kappa_a^2) + \kappa_c^2 (\Delta_2^2 + 3\kappa_a^2)) \omega_2^2 + 2G_2^2 (\Delta - 2\Delta_2) \omega_2^3 + (-\Delta^2 + 4\Delta \Delta_2 - \Delta_2^2 + \kappa_c^2 + 4\kappa_c \kappa_a \\
& + \kappa_a^2) \omega_2^4) + G_1^2 (\gamma_2^2 (\Delta_2^2 \kappa_c - 2\Delta \Delta_2 \kappa_a - \kappa_c \kappa_a^2) + \omega_2^2 (-2\Delta_2^2 \kappa_c + 4\Delta \Delta_2 \kappa_a + 2\kappa_c \kappa_a^2 + (\kappa_c - 2\kappa_a) \omega_2^2))) \\
& - 2J^6 (-G_1^2 \kappa_a (\gamma_2^2 - 2\omega_2^2) + 2(1 + 2\bar{n}_1) \gamma_1 (\gamma_2^2 (\Delta \Delta_2 + \kappa_c \kappa_a) + \omega_2 (G_2^2 \Delta_2 - 2(\Delta \Delta_2 + \kappa_c \kappa_a) \omega_2 + \omega_2^3))) - 2J^2 (-G_1^2 \\
& (\gamma_2^2 (-2\Delta \Delta_2 \kappa_c + \Delta^2 \kappa_a - \kappa_c^2 \kappa_a) (\Delta_2^2 + \kappa_a^2) + 4G_2^2 (1 + 2\bar{n}_2) \gamma_2 \Delta \Delta_2 \omega_2^2 - 2(-2\Delta \Delta_2 \kappa_c + \Delta^2 \kappa_a - \kappa_c^2 \kappa_a) (\Delta_2^2 + \kappa_a^2) \omega_2^2 \\
& + (2\Delta_2 (\Delta + \Delta_2) \kappa_c + (\Delta^2 + 4\Delta \Delta_2 + \Delta_2^2 - \kappa_c^2) \kappa_a - 2\kappa_c \kappa_a^2 + \kappa_a^3) \omega_2^4) + 2(1 + 2\bar{n}_1) \gamma_1 (\gamma_2^2 (\Delta^2 + \kappa_c^2) (\Delta \Delta_2 + \kappa_c \kappa_a) \\
& (\Delta_2^2 + \kappa_a^2) + 2G_2^2 \gamma_2 (\Delta_2^2 (-\Delta + \Delta_2) \kappa_c + \Delta_2 (\Delta (\Delta + \Delta_2) - \kappa_c^2) \kappa_a + (\Delta + \Delta_2) \kappa_c \kappa_a^2 + \Delta \kappa_a^3) \omega_2 + \omega_2 (-2G_2^4 \Delta \Delta_2 \omega_2 \\
& - 2(\Delta^2 + \kappa_c^2) (\Delta \Delta_2 + \kappa_c \kappa_a) (\Delta_2^2 + \kappa_a^2) \omega_2 + (-\Delta \Delta_2 (\Delta^2 - \Delta \Delta_2 + \Delta_2^2) - \Delta_2 (\Delta + \Delta_2) \kappa_c^2 + \kappa_c (\Delta^2 + 4\Delta \Delta_2 + \Delta_2^2 \\
& + \kappa_c^2) \kappa_a - \Delta (\Delta + \Delta_2) \kappa_a^2 + \kappa_c^2 \kappa_a^2 + \kappa_c \kappa_a^3) \omega_2^3 + G_2^2 ((3\Delta^2 \Delta_2 + \Delta_2 \kappa_c^2 + 2\Delta \kappa_c \kappa_a) (\Delta_2^2 + \kappa_a^2) + (\Delta_2 (3\Delta^2 - 2\Delta \Delta_2 \\
& + \Delta_2^2 + \kappa_c^2) - 2(\Delta + 2\Delta_2) \kappa_c \kappa_a + (2\Delta + \Delta_2) \kappa_a^2) \omega_2^2))),
\end{aligned}$$

$$\begin{aligned}
b_7^{(1)} = & \omega_1^2 \omega_2^2 (4G_2^4 (1 + 2\bar{n}_1) \gamma_1 (J^2 \Delta_2 - \Delta (\Delta_2^2 + \kappa_a^2))^2 + (J^4 - 2J^2 (\Delta \Delta_2 + \kappa_c \kappa_a) + (\Delta^2 + \kappa_c^2) (\Delta_2^2 + \kappa_a^2)) \\
& (J^4 (1 + 2\bar{n}_1) \gamma_1 + (2G_1^2 \kappa_c + (1 + 2\bar{n}_1) \gamma_1 (\Delta^2 + \kappa_c^2)) (\Delta_2^2 + \kappa_a^2) - 2J^2 (-G_1^2 \kappa_a + (1 + 2\bar{n}_1) \gamma_1 (\Delta \Delta_2 \\
& + \kappa_c \kappa_a))) \omega_2^2 + 4G_2^2 (J^2 \Delta_2 - \Delta (\Delta_2^2 + \kappa_a^2)) (G_1^2 (1 + 2\bar{n}_2) \gamma_2 (J^2 \Delta_2 - \Delta (\Delta_2^2 + \kappa_a^2)) + (1 + 2\bar{n}_1) \gamma_1 (J^4 \\
& - 2J^2 (\Delta \Delta_2 + \kappa_c \kappa_a) + (\Delta^2 + \kappa_c^2) (\Delta_2^2 + \kappa_a^2)) \omega_2),
\end{aligned} \tag{S84}$$

$$\begin{aligned}
b_0^{(2)} &= 0, \\
b_1^{(2)} &= (1 + 2\bar{n}_2)\gamma_2\omega_2^2, \\
b_2^{(2)} &= \omega_2^2(2G_2^2\kappa_c + (1 + 2\bar{n}_2)\gamma_2(-4J^2 + \gamma_1^2 - 2(\Delta^2 + \Delta_2^2 - \kappa_c^2 - \kappa_a^2 + \omega_1^2))), \\
b_3^{(2)} &= \omega_2^2(6J^4(\gamma_2 + 2\bar{n}_2\gamma_2) + 2G_2^2\kappa_c(\Delta^2 - 2\Delta_2^2 + \kappa_c^2 + 2\kappa_a^2) + (1 + 2\bar{n}_2)\gamma_2(\Delta^4 + \Delta_2^4 - 4\Delta_2^2\kappa_c^2 + \kappa_c^4 + 2\Delta_2^2\kappa_a^2 \\
&\quad + 4\kappa_c^2\kappa_a^2 + \kappa_a^4 + 2\Delta^2(2\Delta_2^2 + \kappa_c^2 - 2\kappa_a^2)) + 2\gamma_1^2(G_2^2\kappa_c - (1 + 2\bar{n}_2)\gamma_2(\Delta^2 + \Delta_2^2 - \kappa_c^2 - \kappa_a^2)) - 4G_1^2(1 + 2\bar{n}_2) \\
&\quad \gamma_2\Delta\omega_1 - 4(G_2^2\kappa_c - (1 + 2\bar{n}_2)\gamma_2(\Delta^2 + \Delta_2^2 - \kappa_c^2 - \kappa_a^2))\omega_1^2 + (1 + 2\bar{n}_2)\gamma_2\omega_1^4 - 2J^2(G_2^2(2\kappa_c - \kappa_a) + 2(1 + 2\bar{n}_2) \\
&\quad \gamma_2(\gamma_2^2 - \Delta^2 + \Delta\Delta_2 - \Delta_2^2 + \kappa_c^2 + \kappa_c\kappa_a + \kappa_a^2 - 2\omega_1^2))\omega_2^2, \\
b_4^{(2)} &= \omega_2^2(-4J^6(\gamma_2 + 2\bar{n}_2\gamma_2) + \gamma_1^2(2G_2^2\kappa_c(\Delta^2 - 2\Delta_2^2 + \kappa_c^2 + 2\kappa_a^2) + (1 + 2\bar{n}_2)\gamma_2(\Delta^4 + \Delta_2^4 - 4\Delta_2^2\kappa_c^2 + \kappa_c^4 + 2(\Delta_2^2 \\
&\quad + 2\kappa_c^2)\kappa_a^2 + \kappa_a^4 + 2\Delta^2(2\Delta_2^2 + \kappa_c^2 - 2\kappa_a^2))) + 8G_1^2(1 + 2\bar{n}_2)\gamma_1\gamma_2\Delta\kappa_c\omega_1 + 2J^4(G_2^2(\kappa_c - 2\kappa_a) + (1 + 2\bar{n}_2)\gamma_2\omega_2 \\
&\quad (3\gamma_1^2 - \Delta^2 - 4\Delta\Delta_2 - \Delta_2^2 + \kappa_c^2 + 4\kappa_c\kappa_a + \kappa_a^2 - 6\omega_1^2)) - 2(G_2^2\kappa_c(-\Delta_2^4 - \kappa_a^2(2\kappa_c^2 + \kappa_a^2) + 2(\kappa_c^2 + 2\kappa_a^2)\omega_1^2 - \omega_1^4 \\
&\quad + 2\Delta_2^2(\kappa_c^2 - \kappa_a^2 - 2\omega_1^2) + 2\Delta^2(\Delta_2^2 - \kappa_a^2 + \omega_1^2)) + (1 + 2\bar{n}_2)\gamma_2(-\kappa_c^2(\Delta_2^4 - \Delta_2^2(\kappa_c^2 - 2\kappa_a^2) + \kappa_a^2(\kappa_c^2 + \kappa_a^2)) \\
&\quad - 2G_1^2\Delta^3\omega_1 + (\Delta_2^4 + \kappa_c^4 + 4\kappa_c^2\kappa_a^2 + \kappa_a^4 + 2\Delta_2^2(-\kappa_c^2 + \kappa_a^2))\omega_1^2 + (\Delta_2^2 - \kappa_c^2 - \kappa_a^2)\omega_1^4 2G_1^2\Delta\omega_1(2\Delta_2^2 + \kappa_c^2 - 2\kappa_a^2 \\
&\quad + \omega_1^2) + \Delta^4(\Delta_2^2 - \kappa_a^2 + \omega_1^2) + \Delta^2(\Delta_2^4 + \kappa_a^4 - 4\kappa_a^2\omega_1^2 + \omega_1^4 + 2\kappa_c^2(-\kappa_a^2 + \omega_1^2) + 2\Delta_2^2(\kappa_c^2 + \kappa_a^2 + 2\omega_1^2))) \\
&\quad + 2J^2(\gamma_1^2(G_2^2(-2\kappa_c + \kappa_a) + 2(1 + 2\bar{n}_2)\gamma_2(\Delta^2 - \Delta\Delta_2 + \Delta_2^2 - \kappa_c^2 - \kappa_c\kappa_a - \kappa_a^2)) + G_2^2(\Delta^2\kappa_a - \kappa_c^2\kappa_a - 2\kappa_c\kappa_a^2 \\
&\quad + \kappa_a^3 + \Delta_2^2(2\kappa_c + \kappa_a) + 2\Delta\Delta_2(\kappa_c + 2\kappa_a) + 4\kappa_c\omega_1^2 - 2\kappa_a\omega_1^2) + 2(1 + 2\bar{n}_2)\gamma_2(\Delta^3\Delta_2 - \kappa_c(\Delta_2^2(-\kappa_c + \kappa_a) + \kappa_a \\
&\quad (\kappa_c^2 + \kappa_c\kappa_a + \kappa_a^2)) - G_1^2\Delta_2\omega_1 + 2(-\Delta_2^2 + \kappa_c^2 + \kappa_c\kappa_a + \kappa_a^2)\omega_1^2 - \omega_1^4 - \Delta^2(\Delta_2^2 + (\kappa_c - \kappa_a)\kappa_a + 2\omega_1^2) + \Delta(\Delta_2^3 \\
&\quad + 2G_1^2\omega_1 + \Delta_2(\kappa_c^2 - 4\kappa_c\kappa_a + \kappa_a^2 + 2\omega_1^2))))),
\end{aligned} \tag{S85}$$

$$\begin{aligned}
b_5^{(2)} &= \omega_2^2(J^8(1 + 2\bar{n}_1)\gamma_2 + (\Delta^2 + \kappa_c^2)(2G_2^2\kappa_c + (1 + 2\bar{n}_1)\gamma_2(\Delta^2 + \kappa_c^2))(\Delta_2^2 + \kappa_a^2)^2 + 2\gamma_1^2(G_2^2\kappa_c(\Delta_2^2(-2\Delta^2 + \Delta_2^2 \\
&\quad - 2\kappa_c^2) + 2(\Delta^2 + \Delta_2^2 + \kappa_c^2)\kappa_a^2 + \kappa_a^4) + (1 + 2\bar{n}_2)\gamma_2(-\Delta_2^2(\Delta^4 - \Delta_2^2\kappa_c^2 + \kappa_c^4 + \Delta^2(\Delta_2^2 + 2\kappa_c^2)) + (\Delta^4 - 2\Delta^2\Delta_2^2 \\
&\quad + 2(\Delta^2 + \Delta_2^2)\kappa_c^2 + \kappa_c^4)\kappa_a^2 + (-\Delta^2 + \kappa_c^2)\kappa_a^4)) - 4G_1^2(1 + 2\bar{n}_2)\gamma_2\Delta(\Delta_2^2(2\Delta^2 + \Delta_2^2 + 2\kappa_c^2) - 2(\Delta^2 - \Delta_2^2 + \kappa_c^2)\kappa_a^2 \\
&\quad + \kappa_a^4)\omega_1 + 4(G_1^4(1 + 2\bar{n}_2)\gamma_2\Delta^2 + G_2^2\kappa_c(\Delta_2^2(2\Delta^2 - \Delta_2^2 + 2\kappa_c^2) - 2(\Delta^2 + \Delta_2^2 + \kappa_c^2)\kappa_a^2 - \kappa_a^4) + (1 + 2\bar{n}_2)\gamma_2(\Delta_2^2 \\
&\quad (\Delta^4 - \Delta_2^2\kappa_c^2 + \kappa_c^4 + \Delta_2^2(\Delta_2^2 + 2\kappa_c^2)) - (\Delta^4 - 2\Delta^2\Delta_2^2 + 2(\Delta^2 + \Delta_2^2)\kappa_c^2 + \kappa_c^4)\kappa_a^2 + (\Delta - \kappa_c)(\Delta + \kappa_c)\kappa_a^4))\omega_1^2 \\
&\quad - 4G_1^2(1 + 2\bar{n}_2)\gamma_2\Delta(\Delta^2 + 2\Delta_2^2 + \kappa_c^2 - 2\kappa_a^2)\omega_1^3 + (2G_2^2\kappa_c(\Delta^2 - 2\Delta_2^2 + \kappa_c^2 + 2\kappa_a^2) + (1 + 2\bar{n}_2)\gamma_2(\Delta^4 + \Delta_2^4 \\
&\quad - 4\Delta_2^2\kappa_c^2 + \kappa_c^4 + 2(\Delta_2^2 + 2\kappa_c^2)\kappa_a^2 + \kappa_a^4 + 2\Delta^2(2\Delta_2^2 + \kappa_c^2 - 2\kappa_a^2)))\omega_1^4 + 4G_1^2\gamma_1\Delta\omega_1(-4(1 + 2\bar{n}_2)\gamma_2\kappa_c(\Delta_2 - \kappa_a) \\
&\quad (\Delta_2 + \kappa_a) + G_2^2(1 + 2\bar{n}_2)\Delta\omega_1) - 2J^6(-G_2^2\kappa_a + 2(1 + 2\bar{n}_2)\gamma_2(\gamma_1^2 + \Delta\Delta_2 + \kappa_c\kappa_a - 2\omega_1^2)) + 2J^4(\gamma_1^2(G_2^2(\kappa_c - 2\kappa_a) \\
&\quad - (1 + 2\bar{n}_2)\gamma_2(\Delta^2 - 4\Delta\Delta_2 + \Delta_2^2 - \kappa_c^2 - 4\kappa_c\kappa_a - \kappa_a^2)) + G_2^2(\Delta_2^2\kappa_c - 2\Delta\Delta_2\kappa_a - \kappa_c\kappa_a^2 - 2(\kappa_c - 2\kappa_a)\omega_1^2) \\
&\quad + (1 + 2\bar{n}_2)\gamma_2(3\Delta^2\Delta_2^2 + \Delta_2^2\kappa_c^2 + 4\Delta\Delta_2\kappa_c\kappa_a + \Delta^2\kappa_a^2 + 3\kappa_c^2\kappa_a^2 - 2G_1^2(\Delta - 2\Delta_2)\omega_1 + 2(\Delta^2 - 4\Delta\Delta_2 + \Delta_2^2 - \kappa_c^2 \\
&\quad - 4\kappa_c\kappa_a - \kappa_a^2)\omega_1^2 + 3\omega_1^4)) - 2J^2(\gamma_1^2(-G_2^2(2\Delta_2(\Delta + \Delta_2)\kappa_c + (\Delta^2 + 4\Delta\Delta_2 + \Delta_2^2 - \kappa_c^2)\kappa_a - 2\kappa_c\kappa_a^2 + \kappa_a^3) \\
&\quad + 2(1 + 2\bar{n}_2)\gamma_2(-\Delta\Delta_2(\Delta^2 - \Delta\Delta_2 + \Delta_2^2) - \Delta_2(\Delta + \Delta_2)\kappa_c^2 + \kappa_c(\Delta^2 + 4\Delta\Delta_2 + \Delta_2^2 + \kappa_c^2)\kappa_a - \Delta(\Delta + \Delta_2)\kappa_a^2 \\
&\quad + \kappa_c^2\kappa_a^2 + \kappa_c\kappa_a^3)) + 4G_1^2(1 + 2\bar{n}_2)\gamma_1\gamma_2(\Delta_2(-\kappa_c + \kappa_a) + \Delta(\kappa_c + \kappa_a))\omega_1 + G_2^2(-(-2\Delta\Delta_2\kappa_c + \Delta^2\kappa_a - \kappa_c^2\kappa_a) \\
&\quad (\Delta_2^2 + \kappa_a^2) + 2(2\Delta_2(\Delta + \Delta_2)\kappa_c + (\Delta^2 + 4\Delta\Delta_2 + \Delta_2^2 - \kappa_c^2)\kappa_a - 2\kappa_c\kappa_a^2 + \kappa_a^3)\omega_1^2 + (2\kappa_c - \kappa_a)\omega_1^4) + 2(1 + 2\bar{n}_2)\gamma_2 \\
&\quad ((\Delta^2 + \kappa_c^2)(\Delta\Delta_2 + \kappa_c\kappa_a)(\Delta_2^2 + \kappa_a^2) - (G_1^2(\Delta_2(3\Delta^2 - 2\Delta\Delta_2 + \Delta_2^2 + \kappa_c^2) - 2(\Delta + 2\Delta_2)\kappa_c\kappa_a + (2\Delta + \Delta_2)\kappa_a^2\omega_1 \\
&\quad + 2(\Delta\Delta_2(\Delta^2 - \Delta\Delta_2 + \Delta_2^2) + \Delta_2(\Delta + \Delta_2)\kappa_c^2 - \kappa_c(\Delta^2 + 4\Delta\Delta_2 + \Delta_2^2 + \kappa_c^2)\kappa_a + (\Delta(\Delta + \Delta_2) - \kappa_c^2)\kappa_a^2 - \kappa_c\kappa_a^3) \\
&\quad \omega_1^2 + G_1^2(2\Delta - \Delta_2)\omega_1^3 + (-\Delta^2 + \Delta\Delta_2 - \Delta_2^2 + \kappa_c^2 + \kappa_c\kappa_a + \kappa_a^2))\omega_1^4))),
\end{aligned} \tag{S86}$$

$$\begin{aligned}
b_6^{(2)} = & \omega_2^2(\gamma_1^2(\Delta^2 + \kappa_c^2)(2G_2^2\kappa_c + (1 + 2\bar{n}_2)\gamma_2(\Delta^2 + \kappa_c^2))(\Delta_2^2 + \kappa_a^2)^2 + 8G_1^2\gamma_1\Delta\omega_1((1 + 2\bar{n}_2)\gamma_2\kappa_c(\Delta_2^2 + \kappa_a^2)^2 \\
& - G_2^2(1 + 2\bar{n}_2)\Delta(\Delta_2 - \kappa_a)(\Delta_2 + \kappa_a)\omega_1) + J^8(1 + 2\bar{n}_2)\gamma_2(\gamma_1^2 - 2\omega_1^2) - 2J^6(\gamma_1^2(-G_2^2\kappa_a + 2(1 + 2\bar{n}_2) \\
& \gamma_2(\Delta(\Delta_2 + \kappa_c\kappa_a)) + 2\omega_1(G_1^2(1 + 2\bar{n}_2)\gamma_2\Delta + G_2^2\kappa_a\omega_1 + (1 + 2\bar{n}_2)\gamma_2\omega_1(-2\Delta\Delta_2 - 2\kappa_c\kappa_a + \omega_1^2))) + 2J^4(\gamma_1^2 \\
& (G_2^2(\Delta_2^2\kappa_c - 2\Delta\Delta_2\kappa_a - \kappa_c\kappa_a^2) + (1 + 2\bar{n}_2)\gamma_2(4\Delta\Delta_2\kappa_c\kappa_a + \Delta^2(3\Delta_2^2 + \kappa_a^2) + \kappa_c^2)(\Delta_2^2 + 3\kappa_a^2))) - 4G_1^2(1 + 2\bar{n}_2) \\
& \gamma_1\gamma_2(\Delta_2\kappa_c - (\Delta + \Delta_2)\kappa_a)\omega_1 + \omega_1(2G_1^2(1 + 2\bar{n}_2)\gamma_2(3\Delta\Delta_2^2 + 2\Delta_2\kappa_c\kappa_a + \Delta\kappa_a^2 + (\Delta - 2\Delta_2)\omega_1^2) + G_2^2\omega_1(-2\Delta_2^2\kappa_c \\
& + 4\Delta\Delta_2\kappa_a + 2\kappa_c\kappa_a^2 + (\kappa_c - 2\kappa_a)\omega_1^2) + (1 + 2\bar{n}_2)\gamma_2\omega_1(-2\Delta_2^2(3\Delta^2 + \kappa_c^2) - 8\Delta\Delta_2\kappa_c\kappa_a - 2(\Delta^2 + 3\kappa_c^2)\kappa_a^2 \\
& + (-\Delta^2 + 4\Delta\Delta_2 - \Delta_2^2 + \kappa_c^2 + 4\kappa_c\kappa_a + \kappa_a^2)\omega_1^2)) - 2\omega_1(4G_1^4(1 + 2\bar{n}_2)\gamma_2\Delta^2(\Delta_2 - \kappa_a)(\Delta_2 + \kappa_a)\omega_1 + 2G_1^2 \\
& (1 + 2\bar{n}_2)\gamma_2\Delta(-(\Delta^2 + \kappa_c^2)(\Delta_2^2 + \kappa_a^2)^2 - (\Delta_2^2(2\Delta^2 + \Delta_2^2 + 2\kappa_c^2) - 2(\Delta^2 - \Delta_2^2 + \kappa_c^2)\kappa_a^2 + \kappa_a^4)\omega_1^2) + \omega_1(G_2^2\kappa_c \\
& (2(\Delta^2 + \kappa_c^2)(\Delta_2^2 + \kappa_a^2)^2 + (\Delta_2^2(-2\Delta^2 + \Delta_2^2 - 2\kappa_c^2) + 2(\Delta^2 + \Delta_2^2 + \kappa_c^2)\kappa_a^2 + \kappa_a^4)\omega_1^2) + (1 + 2\bar{n}_2)\gamma_2((\Delta^2 + \kappa_c^2)^2 \\
& (\Delta_2^2 + \kappa_a^2)^2 + (\Delta_2^2(\Delta^4 - \Delta_2^2\kappa_c^2 + \kappa_c^4 + \Delta^2(\Delta_2^2 + 2\kappa_c^2)) - (\Delta^4 - 2\Delta^2\Delta_2^2 + 2(\Delta^2 + \Delta_2^2)\kappa_c^2 + \kappa_c^4)\kappa_a^2 + (\Delta - \kappa_c) \\
& (\Delta + \kappa_c)\kappa_a^4)\omega_1^2)) - 2J^2(\gamma_1^2(\Delta_2^2 + \kappa_a^2)(2(1 + 2\bar{n}_2)\gamma_2(\Delta^2 + \kappa_c^2)(\Delta\Delta_2 + \kappa_c\kappa_a) + G_2^2(2\Delta\Delta_2\kappa_c - \Delta^2\kappa_a + \kappa_c^2\kappa_a)) \\
& + 4G_1^2\gamma_1\omega_1((1 + 2\bar{n}_2)\gamma_2(\Delta_2^2(-\Delta + \Delta_2)\kappa_c + \Delta_2(\Delta(\Delta + \Delta_2) - \kappa_c^2)\kappa_a + (\Delta + \Delta_2)\kappa_c\kappa_a^2 + \Delta\kappa_a^3) - G_2^2(1 + 2\bar{n}_2) \\
& \Delta\Delta_2\omega_1) - \omega_1(4G_1^4(1 + 2\bar{n}_2)\gamma_2\Delta\Delta_2\omega_1 + 2G_1^2(1 + 2\bar{n}_2)\gamma_2(-(3\Delta^2\Delta_2 + \Delta_2\kappa_c^2 + 2\Delta\kappa_c\kappa_a)(\Delta_2^2 + \kappa_a^2) \\
& - (\Delta_2(3\Delta^2 - 2\Delta\Delta_2 + \Delta_2^2 + \kappa_c^2) - 2(\Delta + 2\Delta_2)\kappa_c\kappa_a + (2\Delta + \Delta_2)\kappa_a^2)\omega_1^2) + \omega_1(G_2^2(-2(-2\Delta\Delta_2\kappa_c + \Delta^2\kappa_a \\
& - \kappa_c^2\kappa_a)(\Delta_2^2 + \kappa_a^2) + (2\Delta_2(\Delta + \Delta_2)\kappa_c + (\Delta^2 + 4\Delta\Delta_2 + \Delta_2^2 - \kappa_c^2)\kappa_a - 2\kappa_c\kappa_a^2 + \kappa_a^3)\omega_1^2) + 2(1 + 2\bar{n}_2)\gamma_2(2(\Delta^2 \\
& + \kappa_c^2)(\Delta\Delta_2 + \kappa_c\kappa_a)(\Delta_2^2 + \kappa_a^2) + (\Delta\Delta_2(\Delta^2 - \Delta\Delta_2 + \Delta_2^2) + \Delta_2(\Delta + \Delta_2)\kappa_c^2 - \kappa_c(\Delta^2 + 4\Delta\Delta_2 + \Delta_2^2 + \kappa_c^2)\kappa_a \\
& + (\Delta(\Delta + \Delta_2) - \kappa_c^2)\kappa_a^2 - \kappa_c\kappa_a^3)\omega_1^2))))), \\
b_7^{(2)} = & \omega_1^2\omega_2^2(4G_1^4(1 + 2\bar{n}_2)\gamma_2(J^2\Delta_2 - \Delta(\Delta_2^2 + \kappa_a^2))^2 + (J^4 - 2J^2(\Delta\Delta_2 + \kappa_c\kappa_a) + (\Delta^2 + \kappa_c^2)(\Delta_2^2 + \kappa_a^2)) \\
& (J^4(1 + 2\bar{n}_2)\gamma_2 + (2G_2^2\kappa_c + (1 + 2\bar{n}_2)\gamma_2(\Delta^2 + \kappa_c^2))(\Delta_2^2 + \kappa_a^2) - 2J^2(-G_2^2\kappa_a + (1 + 2\bar{n}_2)\gamma_2(\Delta\Delta_2 \\
& + \kappa_c\kappa_a))\omega_1^2 + 4G_1^2(J^2\Delta_2 - \Delta(\Delta_2^2 + \kappa_a^2))(G_2^2(1 + 2\bar{n}_1)\gamma_1(J^2\Delta_2 - \Delta(\Delta_2^2 + \kappa_a^2)) + (1 + 2\bar{n}_2)\gamma_2(J^4 \\
& - 2J^2(\Delta\Delta_2 + \kappa_c\kappa_a) + (\Delta^2 + \kappa_c^2)(\Delta_2^2 + \kappa_a^2))\omega_1)). \tag{S87}
\end{aligned}$$

Both analytical and numerical methods are based on the same set of the linearized Langevin equations without further approximations. In our analytical calculations, we use a version based on momentum-damped-mechanical model. However, in the numerical approach, we utilize another version of the model which is based on a rotating-wave-approximation, wherein the loss and damping terms appear symmetrically in the equations of motion for the position and momentum operators. There are physical and mathematical reasons for using both versions. By using the version based on the momentum-damped-mechanical model, we can easily obtain the analytical expressions for effective susceptibilities, cooling rates, and noise spectra. We show that in the high-quality limit, both analytical and numerical results are matched well with each other.

#### IV. GROUND-STATE REFRIGERATION VIA THE EP

In this section, we further study the refrigeration performance of the mechanical resonator, based on both numerical and analytical results of the steady-state average thermal occupation numbers in the vibration for the three cases of: (i) standard cooling; (ii) loss-loss (LL) cooling; (iii) EP cooling.

In Figs. S8(a) and S8(b), we plot the final mean thermal phonon numbers  $n_1^f$  and  $n_2^f$  of the two mechanical resonators as a function of the environmental thermal occupations  $\bar{n}_{\text{th},j}$ , under standard-cooling (see the black curves), LL-cooling (see the blue curves), and EP-cooling (see the red curves) cases. Here we can see that with the increase of thermal noise  $\bar{n}_{\text{th},j}$ , the motional degree of freedom in the EP-cooling case can be effectively cooled; and especially, its cooling performance can be improved up to three orders of magnitude, compared with both standard- and LL-cooling cases. In addition, we find that the cooling performance in the LL-cooling case is much smaller than that in the standard-cooling case, and this confirms that the introduction of an auxiliary passive (active) optical mode can weaken (strengthen) the cooling efficiency of the mechanical resonator.

Physically, our EP system can induce a field-localization effect, which dramatically enhances the absorption rate of the anti-Stokes photons and, meanwhile, extremely reduces the heat-exchange rate between the mechanical vibration and its heat bath [S21–S25]. These results provide the means to protect fragile quantum setups from environmental thermal noise, and pave a way towards noise-tolerant quantum networks.

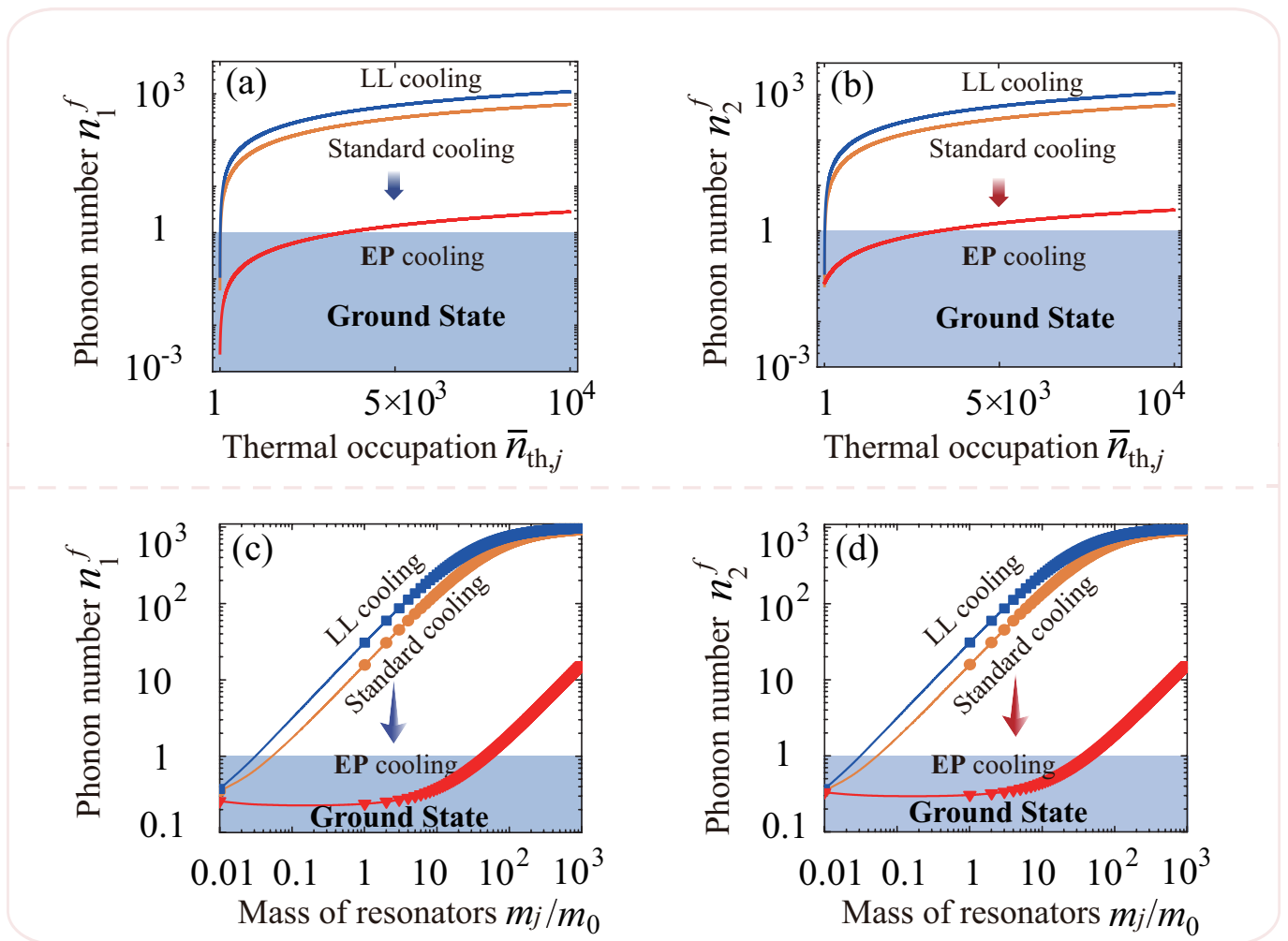


FIG. S8: Final average thermal phonon numbers: (a)  $n_1^f$  of the first mechanical resonator and (b)  $n_2^f$  of the second one versus the environmental thermal occupancies  $\bar{n}_{th,j}$  in the standard-cooling (see the orange curves), loss-loss (LL)-cooling (the blue curves), and EP-cooling (the red curves) cases, when  $m_j = 100$  ng and  $G_j/\kappa_c = 0.05$ . (c)  $n_1^f$  and (d)  $n_2^f$  versus the mechanical-resonator mass ratio  $m_j/m_0$  in the standard-cooling (see the orange curves), LL-cooling (see the blue curves), and EP-cooling (see the red curves) cases, when  $\bar{n}_{th,j} = 10^3$ ,  $m_0 = 100$  ng, and  $G_j/\kappa_c = 0.1$ . The solid curves show the numerical predictions [see Eq. (S30)], while the symbols correspond to our analytical results [see Eq. (S67)]. Clearly, there is an excellent agreement between the numerical and analytical results. Here we set:  $\Delta = \omega_j$  and  $J/\kappa_c = 0.999$ , and other parameters are the same as those in Fig. S3.

For the sake of showing the immunity of the EP-cooling mechanism against the mass of the mechanical resonator, we make a detailed comparison between the standard optomechanical cooling and the EP cooling as a function of the resonator mass, by using both numerical and analytical results of the steady-state average thermal phonon number in the mechanical resonator, as shown in Figs. S8(c) and S8(d). Here, the solid curves are plotted using the numerical results [see Eq. (S30)], while the symbols are based on the analytical predictions [see Eq. (S67)]. Clearly, the numerical results and analytical predictions are matched well with each other, as shown in Figs. S8(c) and S8(d).

In addition, we find that in the standard-cooling case, the optomechanical refrigeration becomes much worse by increasing the resonator mass  $\tilde{m}_j$  (see the upper blue symbols); while in the EP-cooling case, the optomechanical cooling of the mechanical resonator is almost immune to the mass of the mechanical resonator (see the lower symbols). In addition, the EP-cooling technique allows us to reach its quantum ground state, which is very challenging with the standard-cooling schemes. Specifically, in the EP-cooling case, the threshold mass for preserving quantum ground-state cooling has been observed to be more than three orders of magnitude stronger than that in the standard-cooling case. Physically, the net cooling rate is reduced due to the decrease in the light-motion coupling when increasing the mass of the mechanical resonator, while it can be giantly compensated or even amplified by employing the EP-cooling mechanism.

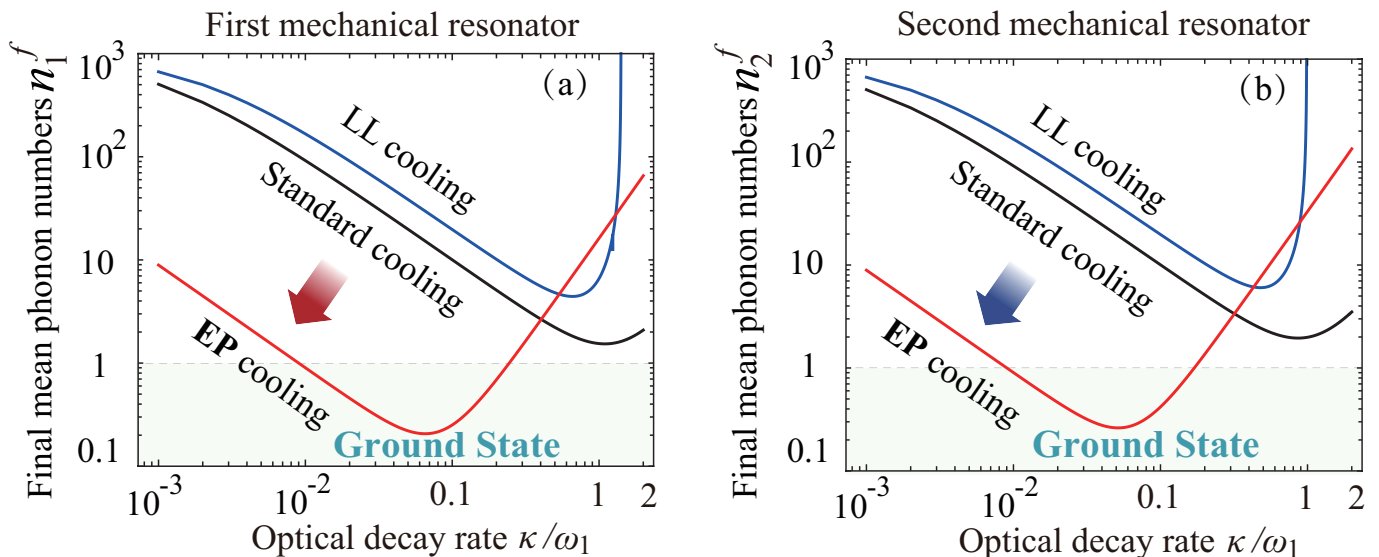


FIG. S9: Final average phonon numbers: (a)  $n_1^f$  of the first mechanical resonator and (b)  $n_2^f$  of the second one, versus the cavity-field decay rate  $\kappa$  in the standard-cooling (see the black curves), loss-loss (LL)-cooling (the blue curves), and EP-cooling (the red curves) cases, when the effective driving detuning takes  $\Delta = \omega_j$  and  $G_j/\kappa_c = 0.1$ . Other parameters are the same as those in Fig. S3.

To better understand the proposed EP-refrigeration mechanism of the system, we also investigate the influence of the cavity-field decay rate  $\kappa$  on the cooling efficiency of the mechanical resonator in the standard-cooling, LL cooling, and EP-cooling cases. Specifically, we consider the case of  $\kappa_c = \kappa_a = \kappa$ , and then, we plot the final average thermal phonon numbers  $n_1^f$  and  $n_2^f$  of the two mechanical resonators as a function of the scaled cavity-field decay rate  $\kappa/\omega_1$  in the standard-cooling, LL cooling, and EP-cooling cases, as shown in Fig. S9. It is shown that, the cooling performance in the EP-cooling case is much better than those in both standard-cooling and LL-cooling cases. This is because the field localization induced by our EP system dramatically enhances the generation rate of the anti-Stokes photons, and meanwhile extremely reduces the heat-exchange rate between the mechanical resonator and its heat reservoir [S21–S25]. These results indicate that, in general, by simply employing the EP, the cooling rate of the mechanical resonator can be giantly amplified and engineered.

In particular, we find that in EP-cooling case, the quantum ground-state refrigeration of the mechanical resonator can be achieved when the system operates in the resolved-sideband regime (i.e.,  $\kappa/\omega_1 \ll 1$ , please see Fig. S9), and this is consistent with a typical resolved-sideband cooling (corresponding to anti-stokes Raman scattering) [S28–S34]. When the phonon sidebands cannot be resolved, the quantum ground-state refrigeration of the vibration is unaccessible in this system (see  $\kappa/\omega_1 > 1$  in Fig. S9). Especially, the cooling performance of the mechanical resonator in the EP-cooling case can be enhanced to be up to nearly ten times, compared with both standard-cooling and LL-cooling cases. In addition, we reveal that in the EP-cooling case, the optimal working parameter of the cavity-field decay rate (corresponding to the minimal value of the final mean thermal phonon numbers) is around  $\kappa/\omega_1 \approx 0.07$ . This optimal value is reached under the combined competition between the optomechanical-cooling rate (i.e., the excitation-energy extraction efficiency through the cavity-field decay channel) and the phonon-sideband resolution condition.

In the quantum refrigeration of our system, the thermal excitations in the mechanical vibration can be effectively extracted by the cooling channels, which are provided by the optomechanical cavity and its vacuum bath. Here, the mechanical motions are thermalized by their thermal baths through the mechanical dissipation channels. As a result, the final average phonon numbers  $n_1^f$  and  $n_2^f$  in the two mechanical resonators depend on their mechanical decay rates  $\gamma_1$  and  $\gamma_2$ . In Fig. S10, we show the final average thermal phonon numbers  $n_j^f$  as a function of the mechanical decay rate  $\gamma_j$  of the  $j$ th mechanical motion, when the system works in the standard-, LL-, and EP-cooling cases. We can see that in these three cases, the final mean thermal phonon numbers  $n_1^f$  and  $n_2^f$  in the two mechanical vibrations increase with increasing the mechanical-motion decay rates  $\gamma_j$ . This is because the thermal energy-exchange rate between the mechanical resonator and its heat baths is faster for a larger value of the mechanical decay rate, and then, the thermal excitations in the heat bath raise the total thermal phonon numbers in the mechanical vibration.

Remarkably, we reveal that the cooling performance of the vibration in the EP-cooling case is much better than those in both standard- and LL-cooling cases, as shown in Fig. S10. Physically, the net-cooling rate is largely reduced due to the increase in the mechanical dissipation strength between the resonator and its thermal bath, while it can

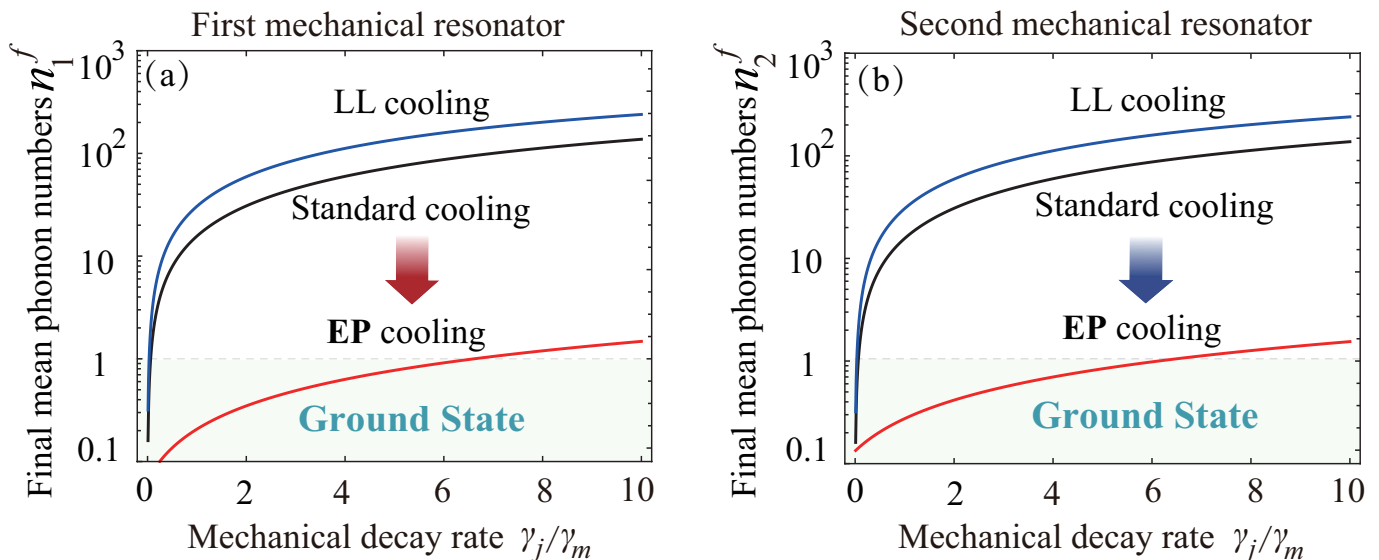


FIG. S10: Final average phonon numbers (a)  $n_1^f$  and (b)  $n_2^f$  versus the mechanical decay rates  $\gamma_j$  in the standard-cooling (see the black curves), loss-loss (LL)-cooling (see the blue curves), and EP-cooling (see the red curves) cases, when the effective driving detuning takes  $\Delta = \omega_j$ ,  $G_j/\kappa_c = 0.1$ , and  $\gamma_m/\omega_1 = 10^{-5}$ . Other parameters are the same as those in Fig. S3.

be giantly compensated or even amplified by utilizing the EP-cooling mechanism. Our findings of the EP-cooling mechanism can pave a route to exploiting quantum ground-state cooling, immune to the mechanical dissipation.

## V. COOLING OPTOMECHANICAL NETWORKS VIA THE EP

Finally, we study in detail the quantum refrigeration performance of optomechanical networks. Specifically, we generalize the EP-cooling mechanism to the ground-state refrigeration of  $N$ -vibration optomechanical networks, which are coupled to a common lossy cavity-field mode  $c$ . For convenience, all the mechanical vibrations are assumed to have the same mechanical decay rates ( $\gamma_j = \gamma_m$  for  $j = 1-N$ ), light-vibration coupling strengths ( $G_j = G$  for  $j = 1-N$ ), mechanical masses [ $m_j = m$  for  $j = 1-N$ ], and bath temperatures [ $T_j = T$  for  $j = 1-N$ ]. In order to seek refrigeration rules for optomechanical networks, we here only consider the case of  $N = 7$ . To explain and visualize the refrigeration performance of the optomechanical networks more clearly, we compare the refrigeration results in the absence of the EP with the cooling results corresponding to the presence of the EP. Figure S11 shows the final mean thermal phonon numbers  $n_j^f$  in these mechanical vibrations as a function of the  $j$ th mechanical motion in both the standard-cooling and EP-cooling cases. We can clearly see that the quantum ground-state refrigeration cannot be realized when the EP is absent ( $J = 0$ , i.e., the standard-cooling case) [see the green columns in Fig. S11]. But in stark contrast to this, the quantum ground-state refrigeration becomes *feasible* [see lower red columns in Fig. S11] by introducing the EP mechanism ( $J \neq 0$ ). This is because the introduced EP leads to compensating and amplifying the net-cooling rate, and makes a giant enhancement for the cooling performance. These results not only open the possibility of further largely suppressing thermal noise in the mechanical-resonator networks, but also pave a route towards the preparation of nonclassical states of motions, e.g., large spatial superpositions or non-Gaussian states (e.g., Schrödinger cat-like states).

In contrast to the previously established demonstrations investigating the exceptional cooling in single-vibration optomechanical platforms [S24, S25], we here focus on the EP-intensive cooling using multi-vibration optomechanical networks showing much richer and more general properties. In particular, our intrinsic motivations are not limited to studying the exceptional refrigeration of the vibration networks by both fully analytical and numerical treatments, but also to overcome a long-standing challenge that quantum ground-state cooling of motions in the regimes of both large mass and high temperature is hard to achieve. This confirms that by simply employing an EP, an ultra-high efficient collective refrigeration can be easily realized, which is robust against both environmental noise and resonator mass, without the need of using any high-cost low-loss materials and noise filters. The resulting exceptional collective

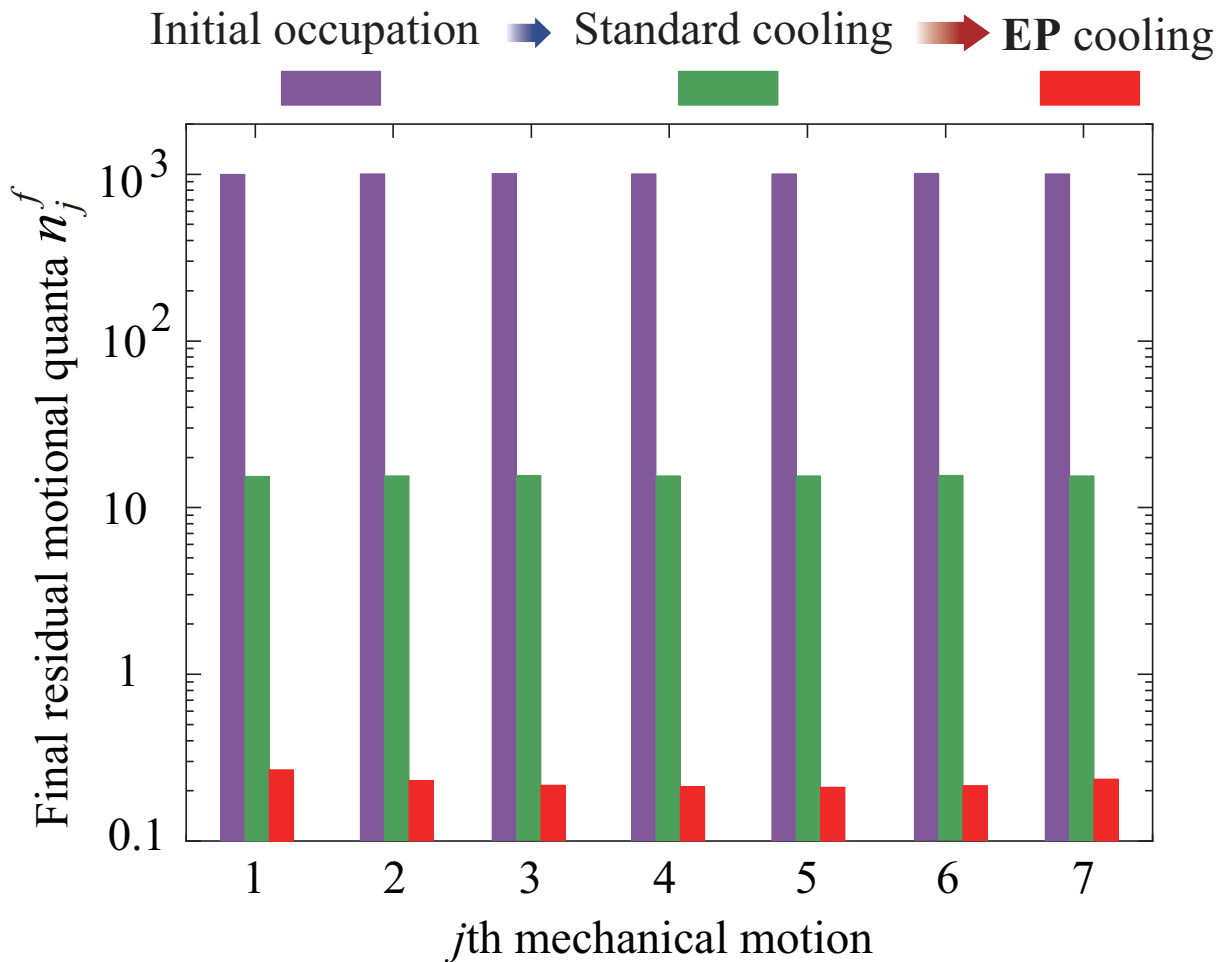


FIG. S11: Final residual thermal phonon numbers  $n_{j \in [1, N]}^f$  for different motional modes. The horizontal axis denotes the frequency dispersion relation of the mechanical resonators with seven independent mechanical frequencies  $(\omega_1, \dots, \omega_7)/\omega_m = 0.7, \dots, 1.3$ . The purple column diagrams are the initial thermal occupations, and the green and red columns denote the final mean phonon numbers in the standard-cooling and EP-cooling cases, respectively. Here  $\Delta = \omega_j$  and  $G_j/\kappa_c = 0.1$ , and other parameters are the same as those in Fig. S3.

refrigeration properties have no counterpart in the previous schemes [S24, S25].

- 
- [S1] C. M. Bender, Making sense of non-Hermitian Hamiltonians, Rep. Prog. Phys. **70**, 947 (2007).  
[S2] Ş. K. Özdemir, S. Rotter, F. Nori, L. Yang, Parity-time symmetry and exceptional points in photonics, Nat. Mater. **18**, 783 (2019).  
[S3] R. El-Ganainy, M. Khajavikhan, D. N. Christodoulides, Ş. K. Özdemir, The dawn of non-Hermitian optics, Commun. Phys. **2**, 37 (2019).  
[S4] F. Minganti, A. Miranowicz, R. Chhajlany, F. Nori, Quantum exceptional points of non-Hermitian Hamiltonians and Liouvillians: The effects of quantum jumps, Phys. Rev. A **100**, 062131 (2019).  
[S5] F. Minganti, A. Miranowicz, R. W. Chhajlany, I. I. Arkhipov, F. Nori, Hybrid-Liouvillian formalism connecting exceptional points of non-Hermitian Hamiltonians and Liouvillians via postselection of quantum trajectories, Phys. Rev. A **101**, 062112 (2020).  
[S6] J. Perma, A. Miranowicz, G. Chimczak, A. Kowalewska-Kudlaszyk, Quantum Liouvillian exceptional and diabolical points for bosonic fields with quadratic Hamiltonians: The Heisenberg-Langevin equation approach, Quantum **6**, 883 (2022).  
[S7] S. Soleymani, Q. Zhong, M. Mokim, S. Rotter, R. El-Ganainy, Ş. K. Özdemir, Chiral and degenerate perfect absorption on exceptional surfaces, Nat. Commun. **13**, 599 (2022).

- [S8] R. Huang, Ş. K. Özdemir, J.-Q. Liao, F. Minganti, L.-M. Kuang, F. Nori, and H. Jing, Exceptional photon blockade: Engineering photon blockade with chiral exceptional points, *Laser Photonics Rev.* **16**, 2100430 (2022).
- [S9] Y. Zuo, R. Huang, L.-M. Kuang, X.-W. Xu, and H. Jing, Loss-induced suppression, revival, and switch of photon blockade, *Phys. Rev. A* **106**, 043715 (2022).
- [S10] L. Feng, Z. J. Wong, R.-M. Ma, Y. Wang, X. Zhang, Single Mode Laser by Parity-Time Symmetry Breaking, *Science* **346**, 972 (2014).
- [S11] H. Hodaei, M.-A. Miri, M. Heinrich, D. N. Christodoulides, M. Khajavikhan, Parity-Time-Symmetric Microring Lasers. *Science* **346**, 975 (2014).
- [S12] W. Chen, Ş. K. Özdemir, G. Zhao, J. Wiersig, L. Yang, Exceptional points enhance sensing in an optical microcavity, *Nature (London)* **548**, 192 (2017).
- [S13] Z. Dong, Z. Li, F. Yang, C.-W. Qiu, J. S. Ho, Sensitive readout of implantable microsensors using a wireless system locked to an exceptional point, *Nat. Electron.* **2**, 335 (2019).
- [S14] Q. Zhong, J. Ren, M. Khajavikhan, D. N. Christodoulides, Ş. K. Özdemir, R. El-Ganainy, Sensing with exceptional surfaces in order to combine sensitivity with robustness, *Phys. Rev. Lett.* **122**, 153902 (2019).
- [S15] Y.-H. Lai, Y.-K. Lu, M.-G. Suh, Z. Yuan, K. Vahala, Observation of the exceptional-point-enhanced Sagnac effect, *Nature (London)* **576**, 65 (2019).
- [S16] M. P. Hokmabadi, A. Schumer, D. N. Christodoulides, M. Khajavikhan, Non-Hermitian ring laser gyroscopes with enhanced Sagnac sensitivity, *Nature (London)*, **576**, 70 (2019).
- [S17] P.-Y. Chen, M. Sakhdari, M. Hajizadegan, Q. Cui, M. M.-C. Cheng, R. El-Ganainy, A. Alù, Generalized parity-time symmetry condition for enhanced sensor telemetry, *Nat. Electron.* **1**, 297 (2018).
- [S18] C. M. Bender, B. K. Berntson, D. Parker, and E. Samuel, Observation of  $PT$  phase transition in a simple mechanical system, *Am. J. Phys.* **81**, 173 (2013).
- [S19] A. Guo, G. J. Salamo, D. Duchesne, R. Morandotti, M. Volatier-Ravat, V. Aimez, G. A. Siviloglou, and D. N. Christodoulides, Observation of  $PT$ -Symmetry Breaking in Complex Optical Potentials, *Phys. Rev. Lett.* **103**, 093902 (2009).
- [S20] H. Jing, Ş. K. Özdemir, X.-Y. Lü, J. Zhang, L. Yang, and F. Nori,  $PT$ -Symmetric Phonon Laser, *Phys. Rev. Lett.* **113**, 053604 (2014).
- [S21] B. Peng, Ş. K. Özdemir, S. Rotter, H. Yilmaz, M. Liertzer, F. Monifi, C. M. Bender, F. Nori, L. Yang, Loss-induced suppression and revival of lasing, *Science* **346**, 328 (2014).
- [S22] B. Peng, Ş. K. Özdemir, F. Lei, F. Monifi, M. Gianfreda, G. Lu Long, S. Fan, F. Nori, C. M. Bender, and L. Yang, Parity-time-symmetric whispering-gallery microcavities, *Nat. Phys.* **10**, 394 (2014).
- [S23] L. Chang, X. Jiang, S. Hua, C. Yang, J. Wen, L. Jiang, G. Li, G. Wang, and M. Xiao, Parity-time symmetry and variable optical isolation in active-passive-coupled microresonators, *Nat. Photon.* **8**, 524 (2014).
- [S24] H. Jing, Ş. K. Özdemir, H. Lü, and F. Nori, High-order exceptional points in optomechanics, *Sci. Rep.*, **7**, 3386 (2017).
- [S25] Y.-L. Liu, and Y.-x. Liu, Energy-localization-enhanced ground-state cooling of mechanical resonator from room temperature in optomechanics using a gain cavity, *Phys. Rev. A* **96** 023812 (2017).
- [S26] E. X. DeJesus and C. Kaufman, Routh-Hurwitz criterion in the examination of eigenvalues of a system of nonlinear ordinary differential equations, *Phys. Rev. A* **35**, 5288 (1987).
- [S27] I. S. Gradshteyn and I. M. Ryzhik, *Table of Integrals, Series, and Products*, 8th ed. (Academic Press, New York, 2014).
- [S28] I. Wilson-Rae, N. Nooshi, W. Zwerger, and T. J. Kippenberg, Theory of Ground State Cooling of a Mechanical Oscillator Using Dynamical Backaction, *Phys. Rev. Lett.* **99**, 093901 (2007).
- [S29] F. Marquardt, J. P. Chen, A. A. Clerk, and S. M. Girvin, Quantum Theory of Cavity-Assisted Sideband Cooling of Mechanical Motion, *Phys. Rev. Lett.* **99**, 093902 (2007).
- [S30] C. Genes, D. Vitali, P. Tombesi, S. Gigan, and M. Aspelmeyer, Ground-state cooling of a micromechanical oscillator: Comparing cold damping and cavity-assisted cooling schemes, *Phys. Rev. A* **77**, 033804 (2008).
- [S31] J. Chan, T. P. Alegre, A. H. Safavi-Naeini, J. T. Hill, A. Krause, S. Groeblacher, M. Aspelmeyer, and O. Painter, Laser cooling of a nanomechanical oscillator into its quantum ground state, *Nature (London)* **478**, 89 (2011).
- [S32] J. D. Teufel, T. Donner, D. Li, J. W. Harlow, M. S. Allman, K. Cicak, A. J. Sirois, J. D. Whittaker, K. W. Lehnert, and R. W. Simmonds, Sideband cooling of micromechanical motion to the quantum ground state, *Nature (London)* **475**, 359 (2011).
- [S33] D. J. Wilson, V. Sudhir, N. Piro, R. Schilling, A. Ghadimi, and T. J. Kippenberg, Measurement-based control of a mechanical oscillator at its thermal decoherence rate, *Nature (London)* **524**, 325 (2015).
- [S34] J. B. Clark, F. Lecocq, R. W. Simmonds, J. Aumentado, J.D. Teufel, Sideband Cooling Beyond the Quantum Limit with Squeezed Light, *Nature (London)* **541**, 20604 (2016).